We thank the referee for their comments and time, which have improved our manuscript in many ways, as detailed below:

This paper uses a set of observations from low-cost, near-surface sensors to examine relationships between CO_2 mole fraction and traffic counts, showing strong relationships at individual sites. They also investigate correlation length scales between different sites and develop a multiple linear regression method to establish relationships between CO_2 mole fraction and the factors that influence it. The methods described appear to give exciting results showing that traffic fuel efficiency can be monitored by combining these methods with traffic count/flow information.

The data and results in this paper are interesting and entirely appropriate for publication in ACP. The major flaw in this paper is that insufficient detail of the methods is given, and mostly only higher level data products (correlation coefficients, MLR coefficients) are given in most places. There are several instances where methods first described in other papers are here described too briefly to be understood without detailed reading of the previous publications. In other cases, figures that are key to understanding the methodology are given only in the supplementary material, and details of the "raw" information that goes into the main figures are lacking. Thus it is difficult to evaluate the robustness of the methods, and readers will have difficulty repeating the analysis or trying it out themselves. ACP doesn't have major length limitations, so the main text should be expanded so that the methodology can be followed. Specific instances are noted in my further comments.

The concepts, data, and written language are all good, but I recommend major revisions to expand the explanations of the methodology and show more of the CO_2 measurements and comparison to the MLR model. This will allow the reviewers and readers to better evaluate the robustness of the methodology.

We appreciate the referee's sentiments with regards to both the significance of our results as well as the shortcomings of our manuscript and we endeavor to improve in the ways suggested. In particular, we have added much more detailed explanations of the methodologies based on previous publications for the convenience of the reader. Due to the extremely high volume of CO_2 observations involved in a multisite, long-term monitoring campaign, it is not always feasible to present the data in its raw form–hence our preference for "higher level" data products that can summarize large quantities of information relatively succinctly. However, an effort has nonetheless been made to incorporate more of the directly observed CO_2 concentrations into the main text wherever possible; case by case explanations of when we did or did not choose to do so are given in response to the specific comments that follow.

Specific comments:

The effect of low-precision measurements is not detailed anywhere in this paper. How does the 0.5 ppm precision impact the results discussed? How is drift in the sensors accounted for, and how will this impact the results, particularly the concept that changes in traffic fuel efficiency could be monitored over time?

The ±0.5 ppm hourly precision has little impact on the results discussed, given that most of said results are obtained after significant averaging. For example, each dark orange point in Fig. 6 represents, on average, 20 hours, giving each a cumulative error of around ±0.13 ppm, which is invisible on the scale of the graph. When we weight each orange point by its specific uncertainty, we actually find a smaller error (11%) in the slope of the resultant linear regression. We have chosen to report the more conservative, non-weighted slope error (17%) in the text. To underscore the insignificance of the measurement precision, we have revised the text as follows:

"The processed 1-minute averages are assumed to have an uncertainty of less than ±4 ppm, which becomes negligible on the averaging timescales used hereafter."

Any long-term drift in the sensors is accounted for via a combination of periodic (i.e., every 12–24 months) laboratory recalibration and a post hoc data treatment based on an independent reference site in the network domain. This procedure allows us to confidently compare measurements taken multiple years apart, thus enabling inter-annual changes in traffic fuel efficiency to be monitored. The exact details of the calibration and post hoc data treatment are provided in Shusterman et al. (2016) and a full repetition of that discussion is beyond the scope of this manuscript.

Although the authors acknowledge that traffic contributes only 40% of CO_2 emissions, they then focus on only traffic emissions in the analysis. While sites very close to major roads will indeed be strongly influenced by the proximal road, sites further from roads will be influenced by multiple roads as well as other anthropogenic sources, AND by biogenic CO_2 sources and sinks. How are these other sources considered? If they are ignored in this analysis, please justify why.

While traffic contributes "only" 40% of the total CO_2 emissions budget for the entire San Francisco Bay Area, this is the single largest source sector in the inventory and the two next largest sectors (industrial/commercial and electricity/co-generation) are often located outside of the urban core studied here. Thus, we safely assume that traffic emissions contribute much more than 40% of the CO_2 emissions in the subset of the overall Bay Area where our sensors are located and focus our subsequent analysis on traffic alone.

We acknowledge that other roads do indeed impact the measurements collected at sites located farther from major highways. We do not require that these roads (or other, non-traffic anthropogenic sources) have negligible influence as a premise for our analysis, however we do find our local CO_2 enhancements and secondary data products to be well correlated with traffic counts on major highways. While ancillary CO_2 sources may account for some of the scatter in our correlations, their insignificance relative to or strong correlation with emissions from major highways is one possible conclusion, rather than a presumption, of our study.

As for the influence of the biosphere, we do not ignore it, but rather adopt data analysis techniques that minimize its importance. Namely, in the multiple linear regression analysis, we separate out the components of the CO_2 signal that are correlated with time of year and temperature (likely to be predictive of biosphere activity) from that which is correlated with day of week (unlikely to be predictive of biosphere activity).

P1 L25: The % of global CO_2 emissions from urban areas varies depending on how it is determined. 70 to 80% is probably a better estimate.

We thank the referee for providing a more accurate range and have updated the text appropriately:

"Currently, an estimated 70–80% of global CO_2 emissions are urban in origin and this fraction is expected to grow as migration to urban areas continues and intensifies with the industrialization of developing nations (United Nations, 2011)."

Section 2.2. Traffic counts. For the sites very close to a particular highway, traffic monitor data for that nearby highway makes sense. For sites that are further from any particular highway, even if traffic is the dominant proximal CO_2 source, surely more than one highway (and local roads as well) will contribute to the signal observed at that site. How are multiple sources accounted for?

We agree that accounting only for the influence of a single highway (rather than multiple highways and/or additional local roads) is a first order approximation of the total traffic emissions influencing a given CO_2 monitor, especially those situated at greater distances from said highway. Interestingly, we nonetheless find this first order approach to produce robust correlations with the observed fluctuations in CO_2. As previously stated in our response to an earlier comment, the predominance of these single highway emissions (and/or their strong correlation with those from other sources) is a possible conclusion, rather than a presumption, of our study.

P3 L31–32; P4 L1–3: Please expand to explain the methodology used here in enough detail to be followed without requiring the reader to refer to the McKain paper. Are these correlation lengths determined using CO_2 mole fraction, or the enhancements in CO_2 relative to the background? Where is the raw data that is used to derive these correlation lengths? Plots of the CO_2 time series should be included (these could go in the supplementary material).

We have expanded the manuscript text to include a more thorough explanation of the methodology used here:

"To quantify the spatial heterogeneity present across the network, we examine the degree of correlation between every possible pairing of sites in a given season as a function of the distance between them, borrowing from a similar analysis used by McKain et al. (2012). For straightforward comparison with the McKain et al. results, we first average the total CO_2 mole fractions to 5-minute resolution. Then, for every pairwise combination of two sites, we perform an ordinary least squares linear regression between the two 5-minute time series and calculate the Pearson correlation coefficient. We repeat this procedure after offsetting the two time series by ±5 minutes, ±10 minutes, etc., allowing for up to a ±3-h lag and choose the optimal r^2 value from the

possible offsets. We plot the thus optimized pairwise correlations as a function of the distance separating the two relevant sites (Figs. 2 and 3) and fit the results to a single term exponential decay on top of a constant background, defined by the mean correlation observed at inter-site distances greater than 20 km."

Given the sheer volume of data used to derive these correlation lengths (3–7 months of data at 5-minute resolution from 28 different sites), we elect to not include CO_2 time series in the supplementary material, as such plots are too visually cramped to be interpreted easily. Instead, we refer interested readers to the Data Availability statement, where we have included a public link to all CO_2 datasets used in this manuscript.

P4 L6–14: Please explain what the correlation lengths should be interpreted to mean. I take it that a shorter correlation length implies more influence of sources close to the sites. Longer length scales would imply more influence of sources further away? The referenced studies are all about pollutant gases, not CO_2–it might be reasonable to expect higher correlations and longer length scales for a long-lived gas like CO_2 with large and varying background.

The referee has correctly inferred our intended interpretation of the correlation lengths, and we have updated the text appropriately to make this explicit:

"The characteristic length scale of this correlation is 2.9 km (defined as the e-folding distance of the exponential fits in Fig. 2; 3.6 km during the day and 2.2 km at night), which we interpret as an indicator of the distance at which various emission sources exert influence over a site's measurements. Shorter correlation lengths indicate sensitivity to near-field emissions, while longer correlation lengths imply sensitivity to far-field phenomena."

We have also edited the discussion of the prior studies of reactive pollutant gases according to the referee's comments:

"In either season, the correlation lengths are, as expected, considerably longer than the previously observed ~100 to 1000-m e-folding distances of reactive urban pollutants that are also lost via chemical pathways (e.g., Zhu et al., 2006; Beckerman et al., 2008; Choi et al., 2014), thus validating the original choice of 2 km as the desirable inter-site separation in the design of the BEACO$_2$N instrument."

P4 L18–19: I don't follow why the daytime correlations imply this information. Please clarify.

We have edited the text and added a figure to clarify our intended interpretation of the daytime correlations:

"However, McKain et al. saw very little correlation after restricting their analysis to daytime hours, even at very short (<5 km) inter-site distances, which implies that daytime observations reflect hyperlocal phenomena only. In contrast, we observe moderate to high correlations during the day, which illustrates that information about emissions and transport phenomena on a variety of scales is preserved. A spatial visualization of the daytime correlation coefficients at four representative winter sites is shown in Fig. 4. We see that PER is well correlated with its neighbors only,

suggesting the presence of local phenomena that do not affect other parts of the network. LCC, however, also exhibits relationships with more distant sites, indicating a sensitivity to more regional-scale (10–30 km) influences. Meanwhile, HRS and OHS each possess at least one near neighbor with whom they are poorly correlated, perhaps due to hyperlocal events specific to those sites. While the region-wide phenomena can be characterized using sparser networks of high-cost, conventional monitoring equipment, the ability to capture these local processes is unique to the high-density approach."

P4 L33: Figure 4, not Fig. 2?

This typographical error has been corrected.

P5 L1–10: It is curious that the amplitude of the diurnal cycle is larger in winter than in summer. The timing of the diurnal pattern shown in Fig. 4 doesn't quite gel with the argument that this is due to the lower/stronger daytime boundary layers. Have the authors considered the influence of biogenic CO_2 fluxes, which may be more important in the rainy winter season in San Francisco than in the summer?

The precise diurnal cycle and relative strength of the summertime vs. wintertime daytime boundary layers in the San Francisco Bay Area are not well understood, so we find this potential explanation of the CO_2 diurnal cycles to be nonetheless plausible if not precisely correct. We do, however, agree that the influence of biogenic CO_2 fluxes may be an important alternative or additional consideration, and have updated the text accordingly:

"This diurnal profile corresponds well with known patterns in traffic emissions–which are largely consistent across seasons–superimposed on diel fluctuations in boundary layer height and/or biosphere activity that vary in timing and magnitude according to the season. Namely, these results might be interpreted to conclude the nighttime boundary layer in the BEACO$_2$N domain to be shallower during the winter months, producing a larger regional increase in response to rush hour traffic. The wintertime layer also appears to expand and re-contract earlier in the day than the summertime layer, resulting in both an earlier minimum and an earlier rise in afternoon–evening concentrations. The larger amplitude of the wintertime diurnal cycle may also reflect the greater influence of daytime photosynthesis and nighttime respiration during the San Francisco Bay Area's rainy winter season."

P5 L 26–35: I pity those commuters who are contributing to high traffic flows at 4 am!

Agreed!

"An alternative analysis using traffic density…" I think I understand that this is an attempt to examine how congested vs free-flowing traffic might change the results? Please clarify.

"We observe a factor of 2 difference in the local CO_2 between congested vs. free-flowing conditions"–which is higher?

The referee has interpreted our reference to traffic density correctly; we subsequently observed congestion to lead to higher local CO_2 enhancements. The text has been updated to provide a clarification with regards to these two comments:

"An alternative analysis using traffic density–obtained by dividing the traffic flow by the average vehicle speed–yields almost identical results (Fig. S5), revealing a factor of 2 increase in the local CO_2 during congestion (high traffic flow/density) relative to free-flowing conditions (low traffic flow/density), similar to that observed by a previous on-road mobile monitoring study by Maness et al. (2015)."

How is the regression slope determined, and how is the uncertainty determined? This needs further detail, particularly because the regression slope is determined not from the full dataset, but from a fit to the median values. The idea that trends in fuel efficiency can be tracked by this method is tantalizing, but the statistics must be demonstrated to be robust.

An explanation of our regression methodology has been added to the text:

"Also shown in Fig. 6 are the median CO_2 concentrations observed in each 500 veh h^{-1} traffic flow increment and the ordinary least squares linear regression through these binned medians."

"The standard error of the slope of the linear regression is calculated as the standard deviation of the model–data CO_2 residuals divided by the square root of the sum of the squared differences between each traffic flow increment and the mean traffic flow."

P6 L5–17: Not enough information is given to understand how these MLRs are constructed and therefore how they can be interpreted. Please expand on the method and provide further details on which factors were most important. On the following page (lines 5–12), there is discussion about how improved resolution of the meteorological datasets would help, but nowhere is the current resolution and limitations of the data explained!

It isn't clear how the "modelled" CO_2 values are determined by this method. Figure S5 is the only place where the MLR and CO_2 values are compared–please include in the main manuscript and expand the discussion of the quality of the model results. Figure S5 is a little misleading–it is easy to make it appear that there is good agreement when the model gets the diurnal cycle roughly right. But it does appear that there are large differences hour by hour. It is hard to tell at the scale shown, but it looks like the model is not capturing the morning rush hour peak very well at all.

We have expanded what was formerly Fig. S5 to include the other four sites and moved it to the main text. In updating Fig. S5 (now Fig. 7), an attempt has also been made to allow for closer examination of model–observation agreement on short timescales by depicting a representative week (rather than an entire month) of data. We have also added a table describing the relative importance of the various MLR factors and updated the text to include a more detailed description of the MLR analysis, the limitations of the meteorological datasets, as well as an explanation and discussion of the model–observation comparison, as follows:

"Briefly, we use an ordinary least squares linear regression to calculate the best fit of the relationship between a site's CO_2 signal and temperature, specific humidity, wind, boundary layer height, time of day, day of week, and time of year. Hourly measurements of temperature, specific humidity, wind speed, and wind direction are taken from a single NOAA Integrated Surface Database weather station at the Port of Oakland International Airport (https://www.ncdc.noaa.gov/isd/) and 3-hour boundary layer heights are provided at 0.125° by 0.125° resolution by the ECMWF's ERA-Interim model (Dee et al., 2011; http://apps.ecmwf.int/datasets/). Although the low spatio-temporal resolution of these datasets limits their ability to capture hyperlocal meteorologies, here we follow the example of de Foy, who was nonetheless able to derive meaningful results from similarly coarse weather products.

The nonlinear relationship between CO_2 concentrations and wind or boundary layer height is captured by dividing these meteorological datasets into quartiles and assigning each observation a value between 0 (at the maximum of the quartile) and 1 (at the minimum) using piecewise linear interpolation. The wind speed quartiles are further subdivided by wind direction and reassigned values of 0–1 accordingly before fitting a linear coefficient to each subset. The time of year is represented as a sum of sines and cosines with annual or semiannual periodicities whose values also vary between 0 and 1 and whose amplitudes are determined by the linear regression. Zeroes and ones are used to designate each hour of each type of day of the week as well. For example, timesteps corresponding to 0800 LT on a Monday may be assigned a 1 while all other timesteps are set to zero before the linear regression is performed. As a result, the MLR factors derived for each of the preceding explanatory variables can be interpreted in units of ppm CO_2. Meanwhile, the temperature and specific humidity variables are treated by calculating their difference from their mean values and dividing by their respective standard deviations before each is fit to CO_2 with a single linear coefficient, which will have units of ppm $^oC^{-1}$ and ppm $(kg_{water}\ kg_{air}^{-1})^{-1}$, respectively.

The independent variable leading to the greatest square of the Pearson correlation coefficient is then combined with each of the remaining variables and a second regression is performed. The two-input combination leading to the largest increase in the correlation coefficient is then combined with each of the remaining variables, and so on, until the addition of a new independent variable no longer increases the r^2 value by at least 0.005.

For this analysis, we use hourly total CO_2 concentrations (the sum of the local and regional components) measured at five sites between 15 February 2017 and 15 February 2018. For each site, the optimal set of explanatory variables and their relative contributions to the correlation coefficient are given in Table 2. Summing the products of each of the MLR factors with their respective independent variables (e.g., time of day, wind speed, etc.) gives the mixing ratio predicted by the MLR model; a representative week of observed and modeled CO_2 concentrations is shown in Fig. 7. We find generally good agreement, with some significant hour-by-hour model–observation differences, especially at RFS. These do not, however, appear to be systematic either in sign or in timing (e.g., the rush hour peak in CO_2 may be poorly modeled on one day but well predicted on another)."

P6 L18–24: How is the intercept of the MLR calculated? Where is the data that shows this? I don't understand how the value of 426 ppm is determined. These MLR coefficients are key to the rest of the interpretation but never clearly explained.

The intercept of the MLR analysis is defined as the modeled CO_2 concentration when all of the input variables possess a value of zero. More details of the MLR analysis have been added in response to previous comments.

P6 L21–24: Why should it be expected that the background is the same in this winter analysis as for the summertime?

The intercept calculated using the MLR analysis is not a wintertime intercept, but rather an annual average intercept, as the MLR analysis spans 15 February 2017 to 15 February 2018. While we do not expect the annual average background to agree perfectly with the summertime background concentration, we find it nonetheless interesting to note that the annual value agrees more closely with the wintertime value than the summertime one.

P6 L32–34: Where do these enhancement percentages come from? I can't see where they are calculated, nor is the CO_2 data for these sites ever shown. I understand that the MLR coefficients are useful for interpreting the data, but the CO_2 mole fractions need to be shown for each site as well.

The weekday enhancements are the maximum difference between Tuesday–Thursday and Sunday hourly MLR factors, expressed as a percentage of the Sunday (lower) factor. We have updated the text appropriately to clarify this point, and have also added a figure depicting the CO_2 mole fractions from which the MLR factors are derived:

"The dependencies on time of day and day of week derived via this method are hypothesized to primarily reflect the changes in emissions, as the influence of the coincident changes in atmospheric dynamics has been at least partially controlled for. For reference, the corresponding Tuesday–Thursday and Sunday diel cycles in the total CO_2 observed at each site are shown in Fig. 9. Indeed, we do observe some of the same intuitive patterns in the linear regression coefficients, such as higher coefficients on weekday mornings corresponding to higher rush hour traffic emissions on those days, but with greater opportunity to differentiate between days of the week, especially around noon when raw concentrations are generally similar. As expected, the Tuesday–Thursday enhancement in the MLR factors is larger at the sites located close to a freeway (e.g., up to 520% higher than the corresponding Sunday MLR factor at FTK) but is less pronounced at LBL (70%), which is farther away from major mobile sources."

P7 L3–4: As in a previous comment–how are the correlation uncertainties determined? This is an exciting result but the uncertainties must be shown to be robust to make it believable.

Please refer to our response to the previous comment concerning correlation uncertainties. We have also added a discussion of the relevant confidence intervals to the text:

"Assuming a steady decrease in emissions of 3.5% per year, one BEACO$_2$N site is therefore sufficiently sensitive to detect such a trend with 68% confidence in as little as 3 years. By leveraging multiple independent sites, even greater confidence and/or shorter timescales could be achieved."

P7 L13–18: The two papers cited only discuss NO_x and particulates, and I suggest that the authors also refer to the literature on CO_2, CO_2ff, or CO ratios, for example:
Miller, J. B., Lehman, S. J., Montzka, S. A., Sweeney, C., Miller, B. R., Wolak, C., Dlugokencky, E. J., Southon, J. R., Turnbull, J. C., and Tans, P. P.: Linking emissions of fossil fuel CO_2 and other anthropogenic trace gases using atmospheric $^{14}CO_2$, J. Geophys. Res., 117, D08302, 2012.
Turnbull, J. C., Sweeney, C., Karion, A., Newberger, T., Lehman, S. J., Tans, P. P., Davis, K. J., Lauvaux, T., Miles, N. L., Richardson, S. J., Cambaliza, M. O., Shepson, P. B., Gurney, K., Patarasuk, R., and Razlivanov, I.: Toward quantification and source sector identification of fossil fuel CO_2 emissions from an urban area: Results from the INFLUX experiment, J. Geophys. Res. Atmos., 120, 292–312, 2015.
Lopez, M., Schmidt, M., Delmotte, M., Colomb, A., Gros, V., Janssen, C., Lehman, S. J., Mondelain, D., Perrussel, O., Ramonet, M., Xueref-Remy, I., and Bousquet, P.: CO, NO_x and $^{13}CO_2$ as tracers for fossil fuel CO_2: results from a pilot study in Paris during winter 2010, Atmos. Chem. Phys., 13, 7343–7358, 2013.
Baker, A. K., Beyersdorf, A. J., Doezema, L. A., Katzenstein, A., Meinardi, S., Simpson, I. J., Blake, D. R., and Sherwood Rowland, F.: Measurements of nonmethane hydrocarbons in 28 United States cities, Atmos. Environ., 42, 170-182, 2008.
Warneke, C., McKeen, S. A., de Gouw, J. A., Goldan, P. D., Kuster, W. C., Holloway, J. S., Williams, E. J., Lerner, B. M., Parrish, D. D., Trainer, M., Fehsenfeld, F. C., Kato, S., Atlas, E. L., Baker, A., and Blake, D. R.: Determination of urban volatile organic compound emission ratios and comparison with an emissions database, J. Geophys. Res., 112, D10S46, 2007.
Nathan, B., Lauvaux, T., Turnbull, J. C., and Gurney, K. R.: Investigations into the use of multi-species measurements for source apportionment of the Indianapolis fossil fuel CO_2 signal, Elem. Sci. Anth., 6, 2018.
Barnes, D. H., Wofsy, S. C., Fehlau, B. P., Gottlieb, E. W., Elkins, J. W., Dutton, G. S., and Montzka, S. A.: Urban/industrial pollution for the New York City–Washington, D. C., corridor, 1996–1998: 1. Providing independent verification of CO and PCE emissions inventories, J. Geophys. Res., 108, 4185, 2003.

We thank the referee for providing such an extensive list of possible references; the Lopez et al. (2013), Nathan et al. (2018), and Turnbull et al. (2015) studies were found to be most relevant to the discussion and have been added to the text.

P8 L1–5: The work in this and previous papers by this group has made huge inroads using low-cost, high-density CO_2 sensors to examine urban emissions, and have shown some clear pathways to where this method is useful. Yet the high-quality, low-density systems favoured by other researchers have also provided exciting results. Indeed, this paper uses high-quality measurements to calibrate and validate the low-cost sensor array. It really isn't helpful to pit the two methods against each other as if only one method is valid. Rather, I suggest that the authors reword to emphasize where the methods are complementary.

We appreciate and agree with this perspective on the complementarity of the two approaches and have revised the text accordingly:

"Most prior studies of urban CO_2 emissions (e.g., McKain et al., 2012; Kort et al., 2013; Wu et al., 2018) have favored sparser networks of high-quality instruments, finding this approach to be better

suited for resolving small trends in total region-wide emissions. It is hypothesized that the ideal monitoring strategy depends on the particular goals and location of a given application, with certain locales and emission sources necessitating high-cost, low-density instrumentation, complemented by other domains where low-cost, high-density platforms are more effective. The potential trade-offs between measurement quality and instrument quantity specific to the San Francisco Bay Area have been investigated previously using an ensemble of observing system simulations by Turner et al. (2016), who found BEACO$_2$N-like observing systems to outperform smaller, higher quality networks in estimating regional as well as more localized emission phenomena there. While Turner et al. saw significant benefits to achieving an instrument precision of 1 ppm, further increases in measurement quality offered little advantage in constraining emissions, especially those from line and point sources."

P8 L5–9: ". . .we do so without the use of computationally intense and heavily parameterized atmospheric transport models." The implication here is that this is the first CO_2-based study to achieve this, whereas in fact a number of studies have gone in this direction. See for example the references given above, and:
LaFranchi, B. W., Pétron, G., Miller, J. B., Lehman, S. J., Andrews, A. E., Dlugokencky, E. J., Miller, B. R., Montzka, S. A., Hall, B., Neff, W., Sweeney, C., Turnbull, J. C., Wolfe, D. E., Tans, P. P., Gurney, K. R., and Guilderson, T. P.: Constraints on emissions of carbon monoxide, methane, and a suite of hydrocarbons in the Colorado Front Range using observations of $^{14}CO_2$, Atmos. Chem. Phys., 13, 11101–11120, 2013.
Turnbull, J. C., Tans, P. P., Lehman, S. J., Baker, D., Chung, Y., Gregg, J. S., Miller, J. B., Southon, J. R., and Zhao, L.: Atmospheric observations of carbon monoxide and fossil fuel CO_2 emissions from East Asia, J. Geophys. Res., 116, D24306, 2011.
McMeeking, G. R., Bart, M., Chazette, P., Haywood, J. M., Hopkins, J. R., McQuaid, J. B., Morgan, W. T., Raut, J. C., Ryder, C. L., Savage, N., Turnbull, K., and Coe, H.: Airborne measurements of trace gases and aerosols over the London metropolitan region. Atmos. Chem. Phys, 11, 5163–5187, 2011.
Ammoura, L., Xueref-Remy, I., Gros, V., Baudic, A., Bonsang, B., Petit, J. E., Perrussel, O., Bonnaire, N., Sciare, J., Chevallier, F.: Atmospheric measurements of ratios between CO_2 and co-emitted species from traffic: a tunnel study in the Paris megacity, Atmos. Chem. Phys., 14, 12871–12882, 2014.

We do not intend to imply that we are the first CO_2-based study to employ simpler models to constrain emissions; we appreciate and acknowledge the important prior work in this vein referenced by the referee. Our intention was rather to contextualize this work relative to the Turner et al. (2016) study referenced in the previous sentence, in which it is suggested that low-cost monitoring frameworks can be fruitfully leveraged using computationally intense atmospheric transport models. The text is simply meant to communicate that we agree low-cost frameworks can be fruitfully leveraged, even without said transport models.

P8 L8–10: The interpretation also requires high quality traffic count information, which is not available everywhere and will be a significant limiting factor.

We agree with the referee that the particular analysis detailed in this manuscript relies on the availability of traffic count information, although we do note that such information does exist for

many metropolitan areas (e.g., http://pems.dot.ca.gov/, http://transportation.austintexas.io/radar/) and ongoing efforts to make these datasets public are progressing in both the academic (https://www.cattlab.umd.edu/) and private (http://www.traffic.com/) sectors. We have, however, added a disclaimer to the manuscript text:

"Furthermore, we show that a multiple linear regression analysis allows the signature of highway traffic to be extracted from sites located throughout the network, enabling trends in mobile emissions to be quantified without specially situated, roadside monitors. Although this approach requires real time traffic count information that is not yet available in all locations, our finding is nonetheless an important result, as deriving and implementing a particular, a priori network layout is a non-trivial task."

FIG7: I suggest showing all data rather than just the median values–Fig. 5 shows that there is a lot of scatter in the individual measurements that shouldn't be ignored.

We believe that a typographical error in the caption for Fig. 7 (now Fig. 10) has led to a misunderstanding about the data that is depicted in said figure. The points shown on these plots are not median values, as the caption originally stated, but rather the entirety of the dataset of MLR coefficients derived to reflect the dependence of the CO_2 concentrations upon time of day and day of week during morning hours (0400–0800 LT); thus there exists no "scatter" to be shown. The caption has been corrected to clarify this point:

"Morning (0400–0800 LT) multiple linear regression coefficients shown as a function of summertime traffic flow; black solid lines indicate the linear regression through the MLR factors (equations given above each subplot) and gray dashed lines show the uncertainty in the regression slope."

References:

Shusterman, A. A., Teige, V. E., Turner, A. J., Newman, C., Kim, J., and Cohen, R. C.: The BErkeley Atmospheric CO_2 Observation Network: initial evaluation, Atmos. Chem. Phys., 16, 13449–13463, doi:10.5194/acp-16-13449-2016, 2016.

Turner, A. J., Shusterman, A. A., McDonald, B. C., Teige, V., Harley, R. A., and Cohen. R. C.: Network design for quantifying urban CO_2 emissions: assessing trade-offs between precision and network density, Atmos. Chem. Phys., 16, 13465–13475, doi:10.5194/acp-16-13465-2016, 2016.

We appreciate the referee's time and feedback, which have resulted in significant improvements to our manuscript, as detailed below:

Shusterman et al. present and analyze results from the low-cost, high-density CO_2 monitoring network BEACO$_2$N to demonstrate that such a network allows investigating hyperlocal sources, e.g., highway traffic, and to track emission changes due to mitigation measures. Key findings, like an experimentally determined correlation length and the strong correlation of local CO_2 enhancements with traffic are important results for the urban GHG research community. Overall, the manuscript is very well written, nicely structured, and concise.

1.) However, some further detail on the methodology would be instructive for other (and future) researchers attempting to use similar approaches, which would ensure that the paper has the best possible impact. The methods applied are properly referenced, but, e.g., the work of de Foy is very recent and some more information might be useful for the reader.

The referee's request for a greater level of detail in our methodological descriptions is a sentiment shared by the other referee as well. We have adjusted the text accordingly, as detailed in response to the specific comments below as well as our other referee response.

2.) Furthermore, the authors do not clearly define the terms used for spatial scales, e.g., "regionwide" (see specific comments). As different groups/communities use different definitions of "regional," it seems imperative that this is added to the manuscript to avoid confusion.

Please see our responses to the specific comments below.

3.) The authors refer to MRV and that this network would/could be useful. While the work described here echoes the concept of MRV, MRV itself, as introduced by the Bali action plan (UNFCCC), seems not to be the best goal. I would argue that providing atmospheric-based constraints on emissions would be very valuable by itself and can enormously help (local) stake-holders without the complications of being integrated into an MRV framework.

We acknowledge that some readers, the referee included, may adhere to a much stricter definition of MRV activities and have removed all references to MRV from the text in favor of language referring to atmospheric-based constraints on emissions more generally; see our responses to the specific comments below for details.

After addressing these comments, I would fully recommend this work for publication in ACP as it is an important advance in the field and will be of great interest to the community.

Specific comments:

P1 L9: Consider adding "at subnational scale" as national CO_2 emissions are usually fairly easy to report based on consumption data compared to, e.g., CFCs, N_2O, or CH_4, and MRV frameworks exist under UNFCCC (e.g., https://unfccc.int/sites/default/files/non-annex_i_mrv_handbook.pdf). For cities MRV has also been developing (e.g., the GHG protocol), but the authors could highlight the added/complementary value of atmospheric information.

We have updated the text to refer to subnational scales and have removed this and all subsequent references to MRV frameworks:

"Urban carbon dioxide comprises the largest fraction of anthropogenic greenhouse gas emissions and yet quantifying urban emissions at subnational scales is highly challenging, as numerous emission sources reside in close proximity within each topographically intricate urban dome."

"To support this effort, there is a clear need for monitoring strategies capable of describing emission changes and attributing those changes to the relevant policy measures (Pacala et al., 2010)."

"However, cities also present the largest atmospheric monitoring challenge in that many disparate emission sources combine with complex topography."

"A considerable amount of emission estimation work has been invested in the development of activity-based emission inventories for selected metropolitan areas […]"

P4 L19: Please give an estimate of what scale "regionwide" refers to.

While the specific sentence to which the referee refers no longer exists in its original form, we have updated the first reference to regional spatial scales in the text to clarify our intended meaning of the term:

"LCC, however, also exhibits relationships with more distant sites, indicating a sensitivity to more regional-scale (10–30 km) influences."

P4 L25: Why did you choose the 10th percentile to define "regional" and not, e.g., the 5th or 20th percentile?

As mentioned in the text, the 10th percentile is chosen "to account for measurement error […] as well as any nearfield draw down from the local biosphere." We note in Sect. 2.1 that Shusterman et al. (2016) found the 1-min mean measurements from the BEACO$_2$N CO_2 monitors to possess an uncertainty of less than ±4 ppm, which amounts to between 5% and 10% of the typical ambient CO_2 signals observed in our urban domain. We therefore adopt the conservative upper limit of 10% to allow for some influence from the biosphere, although a precise quantification of this component of the signal is beyond the scope of this study. Thus, assuming an overall 10% uncertainty in an arbitrarily chosen site's ability to characterize the regional signal, we define the bottom 10th percentile of the observations as our best estimate of this quantity.

The manuscript text has been updated to direct the reader to the reasoning behind this quantity:

"The bottom 10th percentile is chosen (rather than the absolute minimum) to account for measurement error (±4 ppm at 1-min resolution; see Shusterman et al., 2016) as well as any nearfield draw down from the local biosphere; negative values in the local signals are likely attributable to some combination of these effects."

P4 L33: Please correct to "Figure 4."

This typographical error has been corrected.

P5 L3: The daily cycle is mainly driven by boundary layer height dynamics–the local traffic flux is the superimposed fluctuation here, in my opinion. It surely causes a modification, e.g., by causing the morning and evening peaks to be more pronounced. However, different studies in rural regions have largely similar diel cycle shapes (e.g., Garcia et al., 2012 https://www.tandfonline.com/doi/abs/10.3155/1047-3289.58.7.940; Perez et al., 2012 https://www.sciencedirect.com/science/article/pii/S0048969712007498).

We agree with the referee that the traffic flux is the superimposed fluctuation here, and the text as written reflects this sentiment:

"This diurnal profile corresponds well with known patterns in traffic emissions–which are largely consistent across seasons–superimposed on diel fluctuations in boundary layer height and/or biosphere activity that vary in timing and magnitude according to the season."

P5 L6: It seems counter-intuitive that the PBLH changes earlier in winter (also compared to other studies), as more energy is introduced into the system during summer months to break the NBL (as the solar insulation is stronger and the sun rises earlier). Please provide additional data, e.g., PBLH or other atmospheric proxy information in the appendix to support your interpretation.

Unfortunately, there exist no direct PBLH observations in the area with adequate temporal resolution to inform this analysis. Instead we show the median diel cycles in the summer vs. wintertime temperatures and wind speeds observed at the Port of Oakland International Airport's NOAA Integrated Surface Database station (https://www.ncdc.noaa.gov/isd/) below:

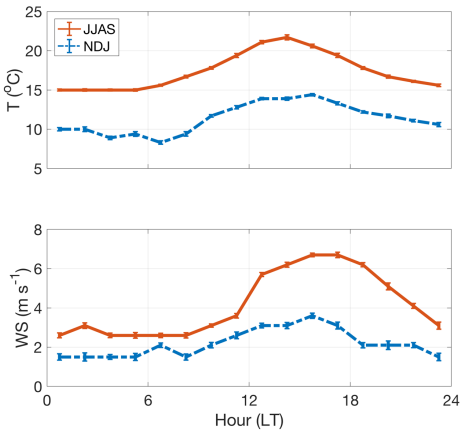

We see that the increases in atmospheric proxies that might be associated with PBLH changes occur at almost identical times of day across seasons, even if the sun rises earlier and more energy is introduced into the system overall during the summer months, as the referee suggests. We do acknowledge, however, that the seasonal differences in PBLH changes are not the only possible explanation for the difference in the diel cycle in regional CO_2 concentrations, and have updated the text to reflect an additional possibility suggested by the other referee:

"Namely, these results might be interpreted to conclude the nighttime boundary layer in the BEACO$_2$N domain to be shallower during the winter months, producing a larger regional increase in response to rush hour traffic. The wintertime layer also appears to expand and re-contract earlier in the day than the summertime layer, resulting in both an earlier minimum and an earlier rise in afternoon–evening concentrations. The larger amplitude of the wintertime diurnal cycle may also reflect the greater influence of daytime photosynthesis and nighttime respiration during the San Francisco Bay Area's rainy winter season."

P5 L32: Why is the other methodology not shown in the supplement and why is this sentence in brackets? Seems to be an interesting finding/information.

We have removed the parentheses around this statement and have added a figure to the supplement that illustrates the results of this alternative methodology.

P5 L34: You could also refer to the large amount of traffic tunnel studies that have similar findings and are very straightforward (no other source besides traffic), e.g., references in https://www.atmos-chem-phys.net/14/12871/2014/acp-14-12871-2014.pdf.

We appreciate the referee's suggestions of additional related studies and believe that such tunnel-based measurement campaigns contribute very important information to mobile emission estimation efforts. However, in the interest of succinctness, we choose to forego a broader discussion of the many analyses that use CO_2 as a baseline against which the concentrations of co-emitted species are normalized and instead limit our discussion to studies that analyze the traffic dependence of CO_2 concentrations in their own right (i.e., Maness et al., 2015).

P5 L35: One question raised would be how long would you have to observe to confirm this 17% trend? Which is answered at P7 L4 for 11–30% emission changes. Consider removing the discussion of the 17% here.

As suggested, we have moved this discussion to occur later in the manuscript.

P6 L15: How exactly are the wind speed quartiles subdivided (and why)? See general comment 1.)

As noted in the text, the wind speed quartiles are subdivided to allow for a "nonlinear relationship" between CO_2 concentrations and this explanatory variable. In Gaussian dispersion modeling, for example, the downwind concentration of a given pollutant is inversely (rather than linearly) proportional to wind speed. Because our regression method is by definition linear, subdividing the wind speeds in this way allows us to decompose more complex mathematical relationships into

linear components. We have updated the text to give more detail regarding the exact methodology of this approach:

"The nonlinear relationship between CO_2 concentrations and wind or boundary layer height is captured by dividing these meteorological datasets into quartiles and assigning each observation a value between 0 (at the maximum of the quartile) and 1 (at the minimum) using piecewise linear interpolation. The wind speed quartiles are further subdivided by wind direction and reassigned values of 0–1 accordingly before fitting a linear coefficient to each subset. The time of year is represented as a sum of sines and cosines with annual or semiannual periodicities whose values also vary between 0 and 1 and whose amplitudes are determined by the linear regression. Zeroes and ones are used to designate each hour of each type of day of the week as well. For example, timesteps corresponding to 0800 LT on a Monday may be assigned a 1 while all other timesteps are set to zero before the linear regression is performed. As a result, the MLR factors derived for each of the preceding explanatory variables can be interpreted in units of ppm CO_2. Meanwhile, the temperature and specific humidity variables are treated by calculating their difference from their mean values and dividing by their respective standard deviations before each is fit to CO_2 with a single linear coefficient, which will have units of ppm $^{o}C^{-1}$ and ppm $(kg_{water}\ kg_{air}^{-1})^{-1}$, respectively.

The independent variable leading to the greatest square of the Pearson correlation coefficient is then combined with each of the remaining variables and a second regression is performed. The two-input combination leading to the largest increase in the correlation coefficient is then combined with each of the remaining variables, and so on, until the addition of a new independent variable no longer increases the r^2 value by at least 0.005."

P6 L26: Why are Mondays and Saturdays not shown in the supplement?

A figure depicting MLR factors derived for Mondays, Fridays, and Saturdays has been added to the supplement.

P6 L29: Could you quantify to which degree the atmospheric dynamics have been controlled for? Claiming that it is "partially controlled for" does not automatically mean that the residual only/primarily reflects emission changes.

Without knowledge of the true emissions within a given site's footprint of sensitivity, we cannot quantify the degree to which atmospheric dynamics have been controlled for. The fact that the MLR factors remaining after "partially" controlling for dynamics may primarily reflect emission changes is a hypothesis rather than a premise of this study, a hypothesis that the discussion goes on to support with a first order, proof-of-concept analysis of the diel cycles in these factors. We have updated the text to clarify the speculative nature of this claim, and also to provide additional detail regarding the diel cycle analysis:

"The dependencies on time of day and day of week derived via this method are hypothesized to primarily reflect the changes in emissions, as the influence of the coincident changes in atmospheric dynamics has been at least partially controlled for. For reference, the corresponding Tuesday–Thursday and Sunday diel cycles in the total CO_2 observed at each site are shown in Fig. 9. Indeed, we do observe some of the same intuitive patterns in the linear regression coefficients,

such as higher coefficients on weekday mornings corresponding to higher rush hour traffic emissions on those days, but with greater opportunity to differentiate between days of the week, especially around noon when raw concentrations are generally similar. As expected, the Tuesday–Thursday enhancement in the MLR factors is larger at the sites located close to a freeway (e.g., up to 520% higher than the corresponding Sunday MLR factor at FTK) but is less pronounced at LBL (70%), which is farther away from major mobile sources."

P7 L4: What is your confidence of the reported detection of such a trend within 2–3 years? 95%? How was this calculated?

The stated uncertainty in the regression slopes (11–30%) is the standard error, i.e., the 68% confidence interval. Assuming that the 35% reduction in CO_2 emissions per vehicle required by fuel efficiency regulation occurs evenly over ~10 years necessitates a 3.5% change in CO_2 emissions per vehicle per year. Thus, with a regression uncertainty of 11%, this 3.5% annual trend is detectable within just over 3 years using the observations from a single site. Even modest improvements in our ability to leverage information from $N > 1$ sites within the network would allow for trend detection with greater confidence and/or shorter timescales if, for example, different sites' observations are found to be sufficiently independent to scale down the uncertainty by $\sqrt{N}$. We have updated the manuscript text to clarify this point, include the re-located discussion of the LAN 17% slope uncertainty, and present the timescale of detection more precisely:

"When we examine the relationship between these multiple linear regression coefficients and morning traffic flow as we did at LAN (Fig. 10), we again find positive correlations. The standard error of the slope of the linear regression is calculated as the standard deviation of the model–data CO_2 residuals divided by the square root of the sum of the squared differences between each traffic flow increment and the mean traffic flow. The uncertainty in the slopes is thus found to be 11–30%, indicating that analysis of a single site could be used to detect as small as 11% changes in average emissions per vehicle, an improvement upon the 17% slope uncertainty calculated for the near-highway LAN site. For reference, under the Corporate Average Fuel Economy standards, the state of California aims to achieve a fleet-wide average fuel economy of 54.5 miles per gallon by the year 2025 (US EPA, 2012), corresponding to a 35% decrease in emissions relative to the 35.5 miles per gallon economy of 2012–2016 model year vehicles. Assuming a steady decrease in emissions of 3.5% per year, one BEACO$_2$N site is therefore sufficiently sensitive to detect such a trend with 68% confidence in as little as 3 years. By leveraging observations from multiple independent sites, even greater confidence and/or shorter timescales could be achieved."

P7 L17: The assumption that plumes can be detected within an urban area should be supported, e.g., by citations. At scales below 1 km^2 it seems that street canyon effects, building disturbances, etc. could play an important role and hinder the application of concepts such as "plumes," see, e.g., Lietzke and Vogt (2013; https://www.sciencedirect.com/science/article/pii/S1352231013002069) that also investigated traffic emissions at street scale.

Previous work using BEACO$_2$N measurements has provided preliminary evidence that plume-like events (if not "plumes" in the strictest sense) can be detected at this scale in urban areas (Kim et al., 2018). These plume-like events are not necessarily representative of a single vehicle's tailpipe, for example, but are nonetheless characterized by a sharp, distinct enhancement above background

concentrations and have been shown to be correlated with average emission factors expected for a given vehicle fleet. We have updated the text to include a reference to this important proof-of-concept study:

"Prior studies have demonstrated a methodology for detecting plume-like events in the BEACO$_2$N NO_x and CO observations (Kim et al., 2018), and the ratio of these species to CO_2 provides a unique signature for each different CO_2 source (e.g., Ban-Weiss et al., 2008; Harley et al., 2005; Lopez et al., 2013; Nathan et al., 2018; Turnbull et al., 2015), allowing subsets of the data record to be directly attributed to specific (e.g., mobile) source types and allowing the relationship between these specific activities and CO_2 mixing ratios to be derived more precisely."

P8 L5: I would suggest reconsidering the wording here, especially as you refer to MRV earlier in the manuscript. This work strongly supports the conclusions of Turner et al. (2016), but it seems you have validated and not verified them.

We appreciate the referee's attention to detail in this case and have updated the text accordingly:

*"*This work thus provides an important data-based validation of the conclusions of Turner et al.'s theoretical analysis."

References:

Kim, J., Shusterman, A. A., Lieschke, K. J., Newman, C., and Cohen, R. C.: The BErkeley Atmospheric CO_2 Observation Network: field calibration and evaluation of low-cost air quality sensors, Atmos. Meas. Tech., 11, 1937–1946, doi:10.5194/amt-11-1937-2018, 2018.

Shusterman, A. A., Teige, V. E., Turner, A. J., Newman, C., Kim, J., and Cohen, R. C.: The BErkeley Atmospheric CO_2 Observation Network: initial evaluation, Atmos. Chem. Phys., 16, 13449–13463, doi:10.5194/acp-16-13449-2016, 2016.

Observing local CO_2 sources using low-cost, near-surface urban monitors

Alexis A. Shusterman[1], Jinsol Kim[2], Kaitlyn J. Lieschke[1], Catherine Newman[1], Paul J. Wooldridge[1], Ronald C. Cohen[1,2]

[1]Department of Chemistry, University of California, Berkeley, Berkeley, 94720, CA, USA
[2]Department of Earth and Planetary Science, University of California, Berkeley, Berkeley, CA, 94720, USA

Correspondence to: Ronald C. Cohen (rccohen@berkeley.edu)

Abstract. Urban carbon dioxide comprises the largest fraction of anthropogenic greenhouse gas emissions but quantifying urban emissions at subnational scales is highly challenging ~~but also the most challenging monitoring, reporting, and verification (MRV) task~~, as numerous emission sources reside in close proximity within each topographically intricate urban dome. In attempting to better understand each individual source's contribution to the overall emission budget, there exists a large gap between activity-based emission inventories and observational constraints on integrated, regional emission estimates. Here we leverage urban CO_2 observations from the BErkeley Atmospheric CO_2 Observation Network ($BEACO_2N$) to enhance, rather than average across or cancel out, our sensitivity to these hyperlocal emission sources. We utilize a method for isolating the local component of a CO_2 signal that accentuates the observed intra-urban heterogeneity and thereby increases sensitivity to mobile emissions from specific highway segments. We demonstrate a multiple linear regression analysis technique that accounts for boundary layer and wind effects and allows for the detection of changes in traffic emissions on scale with anticipated changes in vehicle fuel economy–an unprecedented level of sensitivity for low-cost sensor technologies. The ability to represent trends of policy-relevant magnitudes with a low-cost sensor network has important implications for future applications of this approach, whether as a supplement to sparser existing reference networks or as a substitute in areas where fewer resources are available.

1 Introduction

Initiatives to curb greenhouse gas emissions and thereby reduce the extent of climate change-related damages are gaining momentum from city to global scales (United Nations, 2015). To support this effort, there is a clear need for monitoring~~,~~ ~~reporting, and verification (MRV)~~ strategies capable of describing emission changes and attributing those changes to the relevant policy measures (Pacala et al., 2010). Currently, an estimated 70–80% of global CO_2 emissions are urban in origin and this fraction is expected to grow as migration to urban areas continues and intensifies with the industrialization of developing nations (United Nations, 2011). However, cities also present the largest ~~MRV~~ atmospheric monitoring challenge in that many disparate emission sources combine with complex topography.

A considerable amount of ~~MRV-related~~emission estimation work has been invested in the development of activity-based emission inventories for selected metropolitan areas, such as Indianapolis (Gurney et al., 2012), Paris (Bréon et al., 2015), Los Angeles (Newman et al., 2016), Salt Lake City (Patarasuk et al., 2016), and Toronto (Pugliese et al., 2018), as well as other inventories constructed and maintained by individual air management agencies for internal use. These inventories, when updated regularly, offer the possibility of direct source attribution without the use of computationally intense and/or heavily parameterized atmospheric transport models; they do, however, typically rely on interpolations, generalizations, or proxies to generate the necessary input activity data. The Fuel-based Inventory for Vehicle Emissions ~~inventory~~ developed by McDonald et al. (2014), for example, uses a representative 7 days of highway traffic flow measurements to drive the weekly cycle of CO_2 emissions from mobile sources on roads of all sizes year round. While traffic patterns as well as residential and commercial energy usage are known to vary by day of week (Harley et al., 2005), the specific timing and magnitude of these variations are likely to be heterogeneous in space and time. Mobile emission estimates constructed using an average week of highway observations therefore neglect the impact of anomalous events as well as the variety of vehicle fleets, commute practices, and congestion patterns that occur at the neighborhood level. As knowledge of emission factors and fuel efficiency grows, activity data will become one of the largest sources of uncertainty in bottom-up inventory products.

Ambient atmospheric measurements offer the opportunity to observe nuanced variations in CO_2 emission activities directly without generalizing across space and time. In order to document baseline conditions in and upcoming changes to urban greenhouse gas emissions, surface-level monitoring campaigns in cities using varied approaches are being pursued (e.g., Bréon et al., 2015; Chen et al., 2016; McKain et al., 2012; McKain et al., 2015; Shusterman et al., 2016; Turnbull et al., 2015; and Verhulst et al., 2017). These networks, typically consisting of 2–15 instruments, attempt to constrain and supplement activity-based emission inventories with observation-based estimates. Most previous work on observation-based emission estimates has focused on domain-wide emission totals over monthly to annual timescales (e.g., Kort et al., 2013). This emphasis on integrated signals has led to site selection and data analysis techniques that minimize sensitivity to local emissions, thus discarding a large portion of the information contained in the datasets collected at individual measurement sites and the differences between them (Shusterman et al., 2016; Turner et al., 2016).

We hypothesize that, if trends in the specific, small-scale CO_2 sources implicated in most mitigation strategies are to be resolved from atmospheric monitoring datasets, site-to-site heterogeneity must be sought out and retained. Here we present an initial characterization of the degree of spatial heterogeneity present in an urban monitoring dataset and offer these direct observations of intracity heterogeneities as a possible strategy for providing direct constraints on CO_2 emissions from individual sectors. We provide an initial approach to quantifying changes in the mobile sector and separating the influence of that sector from other emissions.

2 Measurements

2.1 The BErkeley Atmospheric CO_2 Observation Network

The BErkeley Atmospheric CO_2 Observation Network ($BEACO_2N$; see Shusterman et al., 2016) is an ongoing greenhouse gas and air quality monitoring campaign operating in the San Francisco Bay Area since late 2012. The current network is comprised of ~50 "nodes" stationed on top of schools and museums at approximate 2 km--intervals (Fig. 1). The nodes contain a variety of commercially available, low-cost sensor technologies: a Vaisala CarboCap GMP343 for CO_2, a Shinyei PPD42NS for particulate matter, a suite of Alphasense B4 electrochemical devices for O_3, CO, NO, and NO_2, as well as meteorological sensors for pressure, temperature, and relative humidity. Data is collected every 2–10 s and transmitted wirelessly or via an onsite Ethernet connection to a central server, where it is made publicly available in near real time. The distributed low-cost dataset is supplemented by a "supersite" at the RFS location featuring a Picarro G2401 cavity ring-down spectroscopy analyzer for CO_2, CO, and H_2O, a TSI Optical Particle Sizer 3330 for particulate matter, a ThermoFisher Scientific 42i-TL NO_x analyzer for NO and NO_2, a Teledyne 703E photometric calibrator for O_3, a Pandora spectrometer system for total column O_3 and NO_2, a Lufft CHM 15k ceilometer for cloud and aerosol layer height, as well as various instruments for meteorological measurements (i.e., a Vaisala WXT520 weather transmitter, a Campbell Scientific CS500 temperature and relative humidity probe, and a Davis Vantage Pro2 system with a Davis 6410 anemometer and Davis 6450 solar radiation sensor). This high-cost, reference-grade instrumentation serves as a high-accuracy anchor point within the network domain. Atmospheric boundary conditions are monitored by the Bay Area Air Quality Management District's Greenhouse Gas Measurement Program, which maintains its own reference instruments at four background sites to the northwest, east, southeast, and south. A description of the design, deployment, and evaluation of the $BEACO_2N$ approach can be found in Shusterman et al. (2016) and Kim et al. (2018~~7~~).

Here we utilize CO_2 observations from the 20 $BEACO_2N$ sites operating most consistently during the summer and/or winter of 2017 (Table 1), defined as 1 June 2017 through 30 September 2017 and 1 November 2017 through 31 January 2018, respectively. The raw 2--second CO_2 concentrations are averaged to 1--minute means, which are subsequently converted to bias-corrected dry air mole fractions using site-specific meteorological observations and in-network reference measurements (see Shusterman et al., 2016). The processed 1--minute averages are assumed to have an uncertainty of less than ±4 ppm, ~~or ±0.5 ppm at the hourly temporal resolution discussed most often~~which becomes negligible on the averaging timescales used hereafter.

2.2 Traffic Counts

Traffic count data is collected by the California Department of Transportation as part of the Caltrans Performance Measurement System (PeMS; http://pems.dot.ca.gov/). Hourly passenger vehicle flow data (in vehicles per hour) are obtained from the road monitors nearest to the relevant $BEACO_2N$ site with >50% directly observed (as opposed to modeled) data and are summed across all lanes and directions. Due to limited data coverage, in some cases it is necessary to sample road monitors upstream

or downstream of the desired roadway segment; here we assume the sampled traffic conditions to be reasonable approximations of those on the desired segment. The specific monitor IDs used in each analysis are given in Table 1.

3 Results & Discussion

To quantify the spatial heterogeneity present across the network, we examine the degree of correlation between every possible pairing of sites in a given season as a function of the distance between them ~~(Figs. 2 and 3)~~, borrowing from a similar analysis used by McKain et al. (2012). For straightforward comparison with the McKain et al. results, we first average the total CO_2 mole fractions to 5-minute resolution. Then, for every pairwise combination of two sites, we perform an ordinary least squares linear regression between the two 5-minute time series and calculate the Pearson correlation coefficient. We repeat this procedure after offsetting the two time series by ±5 minutes, ±10 minutes, etc., ~~and~~ allowing for up to a ±3-h lag ~~between the two time series before performing a linear regression~~ and choosing the optimal r^2 value from the possible offsets. We plot the thus optimized pairwise correlations as a function of the distance separating the two relevant sites (Figs. 2 and 3) and fit the results to a single term exponential decay on top of a constant background, defined by the mean correlation observed at inter-site distances greater than 20 km.

In the summer months, there appears to be some relationship between the proximity of the sites and the correlation of their observations at all hours, with higher correlations between neighboring sites decaying into more modest, but still significant, correlations at longer inter-site distances. The characteristic length scale of this correlation is 2.9 km (defined as the e-folding distance of the exponential fits in Fig. 2; 3.6 km during the day and 2.2 km at night), which we interpret as an indicator of the distance at which various emission sources exert influence over a site's measurements. Shorter correlation lengths indicate sensitivity to near-field emissions, while longer correlation lengths imply sensitivity to far-field phenomena.

~~-~~The winter months ~~meanwhile~~ exhibit lower pairwise correlations overall and shorter correlation lengths relative to the summertime (2.4 km; 2.6 km during the day and 2.1 km at night). Some portion of the summer–winter differences may be attributable to seasonal differences in dominant wind patterns, although this effect is difficult to disentangle from the slightly different collection of sites sampled during the two seasons; the winter sample, for example, contains fewer pairs with separation lengths less than 5 km, which affects the perceived overall trend. In either season, the correlation lengths are, as expected, considerably longer than the previously observed ~100 to 1000 m e-folding distances of reactive urban pollutants ~~derived by previous studies~~that are also lost via chemical pathways (e.g., Zhu et al., 2006; Beckerman et al., 2008; Choi et al., 2014), ~~however, the correlation length observed here does~~thus validating the original choice of 2 km as the desirable inter-site separation in the design of the BEACO$_2$N instrument.

The 24-hour findings (top panels of Figs. 2 and 3) compare well to those presented by McKain et al., who also documented a decaying but nevertheless persistent correlation with increasing site separation. However, ~~whereas~~ McKain et al. saw very little correlation after restricting their analysis to daytime hours, even at very short (<5 km) inter-site distances, which implies that daytime observations reflect hyperlocal phenomena only. In contrast, we observe moderate to high correlations during the day, which illustrates that information about emissions and transport phenomena on a variety of scales is preserved. ~~This~~

~~suggests that the data record at a particular BEACO$_2$N site contains information about both local and regional emissions and transport phenomena.~~ A spatial visualization of the daytime correlation coefficients at four representative winter sites is shown in Fig. 4. We see that PER is well correlated with its neighbors only, suggesting the presence of local phenomena that do not affect other parts of the network. LCC, however, also exhibits relationships with more distant sites, indicating a sensitivity to more regional-scale (10–30 km) influences. Meanwhile, HRS and OHS each possess at least one near neighbor with whom they are poorly correlated, perhaps due to hyperlocal events specific to those sites. While the region-wide phenomena can be characterized using sparser networks of high-cost, conventional monitoring equipment, the ability to capture these~~o~~ local processes is unique to the high-density approach.

We posit that the true strength of a high-density, surface-level monitoring network lies in its characterization of hyperlocal phenomena unique to a given site or subset of sites. In order to directly examine signals attributable to these specific, local CO_2 emission processes, we separate each site's observations into a "regional" and "local" component. The regional component is, by definition, the same at all sites network-wide, calculated from the bottom 10th percentile of all BEACO$_2$N readings collected during the surrounding 1-~~-~~hour window. The bottom 10th percentile is chosen (rather than the absolute minimum) to account for measurement error (±4 ppm at 1-min resolution; see Shusterman et al., 2016) as well as any near-field draw down from the local biosphere; negative values in the local signals are likely attributable to some combination of these effects. While many different sites contribute to this bottom 10th percentile over the course of the data record, some sites located in close proximity to emission sources are never represented in the bottom 10th percentile and always exhibit some enhancement (i.e., a non-zero local component) over the regional background signal. The regional component is allowed to vary throughout the data record and will therefore reflect domain-wide changes in response to day of week, synoptic weather events, etc.

The diel profiles of the regional signal measured in summer and winter 2017 are shown in Fig. 54, reflecting the typical convolution of background concentrations, emission processes, and dynamics experienced across the entire BEACO$_2$N domain. In both seasons, we see an increase in the regional signal beginning around 0400 local time (LT), followed by a decrease in concentrations at 0800 LT in the winter months and 11~~2~~00 LT in the summer, and another increase in early to late afternoon depending on the season. This diurnal profile corresponds well with known patterns in traffic emissions–which are largely consistent across seasons–superimposed on diel fluctuations in boundary layer height and/or biosphere activity that vary in timing and magnitude according to the season. Namely, these results might be interpreted to conclude the nighttime boundary layer in the BEACO$_2$N domain ~~appears~~ to be shallower during the winter months, producing a larger regional increase in response to rush hour traffic. The wintertime layer also appears to expand~~s~~ and re-contract~~s~~ earlier in the day than the summertime layer, resulting in both an earlier minimum and an earlier rise in afternoon–evening concentrations. The larger amplitude of the wintertime diurnal cycle may also reflect the greater influence of daytime photosynthesis and nighttime respiration during the San Francisco Bay Area's rainy winter season. An analysis of the regional signals calculated for similar periods in 2013 revealed qualitatively similar results (Fig. S1), although it should be noted that the 2013 analysis uses observations from a significantly different subset of sites in the BEACO$_2$N network.

We isolate the local signals by subtracting the network-wide regional component from the data record at each site. Median 1-minute local CO_2 signals range from 0.3 to 40.2 ppm during the day (1100–1800 LT) and 1.1 to 38.5 ppm at night (2100–0400 LT) during the summer months, although the distributions are skewed, with the 10th to 90th percentile ranges stretching from -2.4 to 69.0 ppm during the day and -2.0 to 45.0 ppm at night. During the winter months, the daytime medians range from 3.6 ppm to 34.8 ppm (-7.0 to 90.8 ppm 10th to 90th percentile range) and -0.8 ppm to 58.7 ppm (-15.0 to 90.6 ppm 10th to 90th percentile range) at night. A full picture of the overall distributions is shown in Figs. S2 and S3, confirming a much greater frequency of high CO_2 concentrations during the winter months. In both seasons, the distribution of the local enhancements is typically unimodal with a heavy right-hand tail, although some sites exhibit more complex bi- or multi-modal distributions.

By definition, we expect these local signals to represent a unique combination of emission sources and atmospheric dynamics specific to a given site. Mobile sources are estimated to comprise approximately 40% of the San Francisco Bay Area's annual CO_2 emissions (Claire et al., 2015) and are likely to represent an even larger fraction within the urban core, where electricity and co-generation sources are less abundant. However, as noted in the discussion of the regional signals above, direct observation of the magnitude and variation of traffic emissions via ambient CO_2 concentrations is complicated by the coincident variation in turbulent mixing and boundary layer height as the earth's surface warms and cools at sunrise and sunset (Fig. S4).

In order to more directly examine the relationship between highway traffic flow and urban CO_2 concentrations, we begin by analyzing the subset of observations collected between 0400 and 0800 LT at the LAN site, located less than 40 m from Interstate 880. During this period, traffic emissions are high, but the boundary layer is relatively shallow, thus increasing the sensitivity of the surface-level monitor to the traffic signal. The resultant strong positive correlation between rush hour traffic flow and local CO_2 concentrations is shown in Fig. 6~~5, along with the median CO_2 concentrations observed in each 500 veh h^{-1} traffic flow increment and the linear regressions through these binned medians. (~~. An alternative analysis using traffic density–obtained by dividing the traffic flow by the average vehicle speed–yields almost identical results (Fig. S5), ~~)~~revealing ~~We observe~~ a factor of 2 ~~difference~~ increase in local CO_2 ~~between congested vs. free-flowing conditions~~during congestion (high traffic flow/density) relative to free-flowing conditions (low traffic flow/density), similar to that observed by a previous on-road mobile monitoring study by Maness et al. (2015). Also shown in Fig. 6 are the median CO_2 concentrations observed in each 500 veh h^{-1} traffic flow increment and the ordinary least squares linear regression through these binned medians. ~~The uncertainty in the slope of the linear regression is 17%, indicating that this analysis of a single site could be used to detect 17% changes in average emissions per vehicle. For reference, under the Corporate Average Fuel Economy standards, the state of California aims to achieve a fleet-wide average fuel economy of 54.5 miles per gallon by the year 2025 (US EPA, 2012), corresponding to a 35% decrease in emissions relative to the 35.5 miles per gallon economy of 2012–2016 model year vehicles.~~

In addition to this first-order sensitivity to vehicle emissions at the near-roadway LAN site, we find that ~~policy-relevant~~relatively subtle emission changes can also be detected using nodes stationed greater distances from the highway by controlling for the impacts of dispersion. To do so, we decompose the CO_2 signals into terms that represent the influence of

meteorology and emissions separately via a multiple linear regression approach analogous to that described by de Foy (2018). Briefly, ~~linear coefficients describing~~ we use an ordinary least squares linear regression to calculate the best fit of the relationship between~~of~~ a site's CO_2 signal and~~to~~ temperature, specific humidity, wind, boundary layer height, time of day, day of week, and time of year~~ are derived in an iterative, compounding fashion, with the variable leading to the greatest increase in the square of the Pearson correlation coefficient being added to the regression until the addition of a new variable no longer increases the r^2 value by at least 0.005.~~. Hourly measurements of t~~T~~emperature, specific humidity, wind speed, and wind direction are taken from~~ the Port of Oakland International Airport weather station maintained by the~~ a single NOAA Integrated Surface Database weather station at the Port of Oakland International Airport (https://www.ncdc.noaa.gov/isd/) and 3-hour boundary layer heights are provided at 0.125° by 0.125° resolution by the ECMWF's ERA-Interim model (Dee et al., 2011; http://apps.ecmwf.int/datasets/). Although the low spatio-temporal resolution of these datasets limits their ability to capture hyperlocal meteorologies, here we follow the example of de Foy, who was nonetheless able to derive meaningful results from similarly coarse weather products.

The nonlinear relationship between CO_2 concentrations and wind or boundary layer height is captured by dividing these meteorological datasets into quartiles and assigning each observation a value between 0 (at the maximum of the quartile) and 1 (at the minimum) using piecewise linear interpolation. ~~deriving a linear coefficient for each subset.~~ The wind speed quartiles are further subdivided by wind direction and reassigned values of 0–1 accordingly before fitting a linear coefficient to each subset. The time of year is represented as a sum of sines and cosines with annual or semiannual periodicities whose values also vary between 0 and 1 and whose amplitudes are determined by the linear regression. Zeroes and ones are used to designate each hour of each type of day of the week as well. For example, timesteps corresponding to 0800 LT on a Monday may be assigned a 1 while all other timesteps are set to zero before the linear regression is performed. As a result, the MLR factors derived for each of the preceding explanatory variables can be interpreted in units of ppm CO_2. Meanwhile, the temperature and specific humidity variables are treated by calculating their difference from their mean values and dividing by their respective standard deviations before each is fit to CO_2 with a single linear coefficient, which will have units of ppm $^oC^{-1}$ and ppm $(kg_{water}\ kg_{air}^{-1})^{-1}$, respectively.

The independent variable leading to the greatest square of the Pearson correlation coefficient is then combined with each of the remaining variables and a second regression is performed. The two-input combination leading to the largest increase in the correlation coefficient is then combined with each of the remaining variables, and so on, until the addition of a new independent variable no longer increases the r^2 value by at least 0.005.

For this analysis, we use hourly total CO_2 concentrations (the sum of the local and regional components) measured at five sites between 15 February 2017 and 15 February 2018. For each site, the optimal set of explanatory variables and their relative contributions to the correlation coefficient are given in Table 2. Summing the products of each of the MLR factors with their respective independent variables (e.g., time of day, wind speed, etc.) gives the mixing ratio predicted by the MLR model; a representative ~~comparison~~ week of ~~the~~ observed and modeled ~~results~~ CO_2 concentrations ~~at the LCC site~~ is shown in Fig. 7~~S5~~. We find generally good agreement, with some significant hour-by-hour model–observation differences, especially at RFS.

These do not, however, appear to be systematic either in sign or in timing (e.g., the rush hour peak in CO_2 may be poorly modeled on one day but well predicted on another).

Additionally, ~~T~~the intercept of the multiple linear regression provides an estimate of the average background CO_2 concentration observed at a given site over the entire analysis period; here we find a mean intercept of 426 ppm across the five sites. This is considerably higher than the average 407 ppm regional signal calculated for the summer months using the bottom 10th percentile method described above, but in good agreement with the average wintertime regional signal (425 ppm).

Multiple linear regression coefficients are derived for each hour of the day during five types of days of the week (Mondays, Tuesdays through Thursdays, Fridays, Saturdays, and Sundays); for clarity, Fig. ~~8~~6 shows the regression coefficients for Tuesdays through Thursdays and Sundays. Other days of the week are shown in Fig. S6. These MLR "factors" signify the average CO_2 enhancement or depletion (in ppm) uniquely associated with a particular hour of a particular day of the week. The dependencies on time of day and day of week derived via this method are hypothesized to primarily reflect the changes in emissions, as the influence of the coincident changes in atmospheric dynamics has been at least partially controlled for. For reference, the corresponding Tuesday–Thursday and Sunday diel cycles in the total CO_2 observed at each site are shown in Fig. 9. Indeed, we do observe some of the same intuitive patterns in the linear regression coefficients, such as higher coefficients on weekday mornings corresponding to higher rush hour traffic emissions on those days, but with greater opportunity to differentiate between days of the week, especially around noon when raw concentrations are generally similar. As expected, the ~~weekday~~ Tuesday–Thursday enhancement in the MLR factors is larger at the sites located close to a freeway (e.g., up to 520% higher than the corresponding Sunday MLR factor at FTK) but is less pronounced at LBL (70%), which is farther away from major mobile sources. For reference, the 1 km by 1 km FIVE mobile emission inventory developed for the San Francisco Bay Area by McDonald et al. (2014) predicts a ~210% weekday enhancement on average, peaking around 0500 LT, much earlier in the day than is observed here.

When we examine the relationship between these multiple linear regression coefficients and morning traffic flow as we did at LAN (Fig. 10~~7~~), we again find positive correlations. The standard error of the slope of the linear regression is calculated as the standard deviation of the model–data CO_2 residuals divided by the square root of the sum of the squared differences between each traffic flow increment and the mean traffic flow. The uncertainty in the slopes is thus found to be 11–30%, indicating that analysis of a single site could be used to detect as small as 11% changes in average emissions per vehicle, an improvement upon the 17% slope uncertainty calculated for the near-highway LAN site. For reference, under the Corporate Average Fuel Economy standards, the state of California aims to achieve a fleet-wide average fuel economy of 54.5 miles per gallon by the year 2025 (US EPA, 2012), corresponding to a 35% decrease in emissions relative to the 35.5 miles per gallon economy of 2012–2016 model year vehicles. Assuming a steady decrease in emissions of 3.5% per year, one BEACO$_2$N site is therefore sufficiently sensitive to detect such a trend with 68% confidence in as little as 3 years. By leveraging multiple independent sites, even greater confidence and/or shorter timescales could be achieved.~~enabling the detection of 11–30% changes in emissions. This is sufficient sensitivity to detect and monitor future increases in the fuel efficiency of the California passenger vehicle fleet with a record as short as 2–3 years.~~

It is likely that even greater sensitivity could be achieved with more accurate meteorological datasets. While the single weather station and relatively coarse (0.125° by 0.125°) reanalysis product we use here may be adequate to represent the meteorological conditions across some domains, the San Francisco Bay Area is at the high end of complexity in terms of terrain and microclimatology. Higher resolution boundary layer heights and neighborhood-specific wind observations may improve the results of our multiple linear regression, but these types of measurements are rarely available on the spatial scale of the BEACO$_2$N instrument and are difficult to simulate with accuracy (Jiménez et al., 2013; Banks et al., 2016). In future work, high-density networks like BEACO$_2$N may therefore be useful not just in source attribution but also in providing a much needed observational constraint on our understanding of near-surface transport.

Future work will also make use of the ancillary datasets provided by the BEACO$_2$N platform, such as the concurrent NO_x and CO concentrations. Prior studies have demonstrated a methodology for detecting plume-like events in the BEACO$_2$N NO_x and CO observations (Kim et al., 2018), and t~~T~~he ratio of these species to CO_2 provides a unique signature for each different CO_2 source (e.g., Ban-Weiss et al., 2008; Harley et al., 2005; Lopez et al., 2013; Nathan et al., 2018; Turnbull et al., 2015), allowing ~~"plumes" or other~~ subsets of the data record to be directly attributed to specific (e.g., mobile) source types and allowing the relationship between these specific activities and CO_2 mixing ratios to be derived more precisely. With such a precise methodology for converting between emissions and concentrations, subtler inter-annual trends in emissions could be detected, for example changes in vehicle emissions following construction of new housing.

4 Conclusions

We have described the heterogeneity measured at the individual sites of a high-density, surface-level urban CO_2 monitoring network. Networkwide, correlation length scales are found to be slightly longer during daytime during the summer, and generally shorter during winter months, but falling in the range of values reported previously based on other stationary observation networks and mobile monitoring campaigns. High near-field correlations are thought to be driven by shared sensitivity to local emission events, while moderate far-field correlations reflect regional episodes, suggesting that a given site's data record is likely a convolution of both phenomena. We therefore present a methodology for separating the observed CO_2 concentrations into local and regional components and observe distinct distributions (i.e., unimodal vs. bimodal) of local CO_2 enhancements within single neighborhoods. A clear relationship is seen between morning rush hour traffic counts and local CO_2 concentrations, allowing for the detection of changes in vehicle emissions within 2–3 years, if those changes proceed at a rate consistent with policy objectives.

Most p~~P~~rior ~~publications~~ studies of urban CO_2 emissions (e.g., McKain et al., 2012; Kort et al., 2013; Wu et al., 2018) have favored sparser networks of high-quality instruments, finding this approach to be better suited for resolving trends in total region-wide emissions. It is hypothesized that the ideal monitoring strategy depends on the particular goals and location of a given application, with certain locales and emission sources necessitating high-cost, low-density instrumentation, complemented by other domains where low-cost, high-density platforms are more effective. ~~criticizing high-density, low-cost approaches as either: (a) providing redundant constraints on total urban emissions, (b) offering information on CO_2 sources in~~

~~their immediate surroundings only, or (c) possessing insufficient accuracy to resolve small emission trends.~~ The ~~ideal~~ potential trade-offs between measurement quality and instrument quantity specific to the San Francisco Bay Area haves~~s~~ been investigated previously using an ensemble of observing system simulations by Turner et al. (2016), who found BEACO$_2$N-like observing systems to outperform smaller, higher quality networks in estimating regional as well as more localized emission phenomena there. While Turner et al. saw significant benefits to achieving an instrument precision of 1 ppm, further increases in measurement quality offered little advantage in constraining emissions, especially those from line and point sources.

This work thus provides an important data-based ~~verification~~ validation of the conclusions of Turner et al.'s theoretical analysis. Not only do we demonstrate the ability of low-cost sensors to sufficiently constrain policy-relevant trends in line source (i.e., highway traffic) emissions, but we do so without the use of computationally intense and heavily parameterized atmospheric transport models. Furthermore, we show that a multiple linear regression analysis allows the signature of highway traffic to be extracted from sites located throughout the network, enabling trends in mobile emissions to be quantified without specially situated, roadside monitors. Although this approach requires real time traffic count information that is not yet available in all locations, our finding is ~~This~~ nonetheless~~is~~ an important result, as deriving and implementing a particular, a priori network layout is a non-trivial task. Domain-specific transport patterns prevent the development of general principles of optimal sensor placement, and, even if ideal locations can be identified, cooperation from facilities in the area cannot be guaranteed. By establishing for the first time that an ad hoc, opportunistic sensor siting approach can nonetheless provide sensitivity to emission sources of interest, we thus improve the prospects for widespread adoption of distributed monitoring systems in the future.

Progress toward evaluating the capabilities and proper ~~leverage~~ use of low-cost sensors has particular relevance for nations with rapidly developing economies, where CO_2 emissions are increasing much faster than the resources needed to monitor them by conventional means. Domestically, citizen science and environmental justice groups are also adopting these technologies (Snyder et al., 2013) as an economically accessible means of advocating for greater public health and ecological wellbeing. While the specific correlation lengths and emission estimates we derive here are unique to the San Francisco Bay Area domain, the sensor performance capabilities and data analysis techniques we outline provide guidance more generally to any future studies attempting to interpret similar datasets around the world. High-resolution surface networks enabled by low-cost technologies offer a unique opportunity to provide ground truth constraints on difficult-to-model near-surface dynamics as well as on the individual CO_2 sources and sinks that comprise the strategic backbone of greenhouse gas mitigation regulation.

5 Data Availability

All BEACO$_2$N CO_2 observations used in this analysis can be downloaded at doi:10.5281/zenodo.1206983. Traffic counts are available on the California Department of Transportation website (http://pems.dot.ca.gov/), wind, temperature, and humidity observations are available on the NOAA Integrated Surface Database website (http://www.ncdc.noaa.gov/isd/), and boundary layer heights are available on the ECMWF website (http://apps.ecmwf.int/datasets/).

Acknowledgements. This work was funded by the National Science Foundation (1035050; 1038191), the National Aeronautics and Aerospace Administration (NAS2-03144), the Bay Area Air Quality Management District (2013.145), and the Environmental Defense Fund. Additional support was provided by a NSF Graduate Research Fellowship to AAS, a Kwanjeong Lee Chonghwan Educational Fellowship to JK, and a Hellman Fund Fellowship to KJL. We acknowledge the use of datasets maintained by the California Department of Transportation, the National Oceanic and Atmospheric Administration, as well as the European Centre for Medium-Range Weather Forecasts.

References

Banks, R. F., Tiana-Alsina, J., Baldasano, J. M., Rocadenbosch, F., Papayannis, A., Solomos, S., and Tzanis, C. G.: Sensitivity of boundary-layer variables to PBL schemes in the WRF model based on surface meteorological observations, lidar, and radiosondes during the HygrA-CD campaign, Atmos. Res., 176, 185–201, doi:10.1016/j.atmosres.2016.02.024, 2016.

Ban-Weiss, G. A., McLaughlin, J. P., Harley, R. A., Lunden, M. M., Kirchstetter, T. W., Kean, A. J., Strawa, A. W., Stevenson, E. D., and Kendall, G. R.: Long-term changes in emissions of nitrogen oxides and particulate matter from on-road gasoline and diesel vehicles, Atmos. Environ., 42, 220–232, doi:10.1016/j.atmosenv.2007.09.049, 2008.

Beckerman, B., Jerrett, M., Brook, J. R., Verma, D. K., Arain, M. A., and Finkelstein, M. M.: Correlation of nitrogen dioxide with other traffic pollutants near a major expressway, Atmos. Environ., 42, 275–290, doi:10.1016/j.atmosenv.2007.09.042, 2008.

Bréon, F. M., Broquet, G., Puygrenier, V., Chevallier, F., Xueref-Remy, I., Ramonet, M., Dieudonné, E., Lopez, M., Schmidt, M., Perrussel, O., and Ciais, P.: An attempt at estimating Paris area CO_2 emissions from atmospheric concentration measurements, Atmos. Chem. Phys., 15, 1707–1724, doi:10.5194/acp-15-1707-2015, 2015.

Brown, E. G.: 2016 ZEV action plan: an updated roadmap toward 1.5 million zero-emission vehicles on California roadways by 2025, Governor's Interagency Working Group on Zero-Emission Vehicles, Sacramento, CA, USA, 2016.

Chen, J., Viatte, C., Hedelius, J. K., Jones, T., Franklin, J. E., Parker, H., Gottlieb, E. W., Wennberg, P. O., Dubey, M. K., and Wofsy, S. C.: Differential column measurements using compact solar-tracking spectrometers, Atmos. Chem. Phys., 16, 8479–8498, doi:10.5194/acp-16-8479-2016, 2016.

Choi, W., Winer, A. M., and Paulson, S. E.: Factors controlling pollutant plume length downwind of major roadways in nocturnal surface inversions, Atmos. Chem. Phys., 14, 6925–6940, doi:10.5194/acp-14-6925-2014, 2014.

Claire, S. J., Dinh, T. M., Fanai, A. K., Nguyen, M. H., and Schultz, S. A.: Bay Area emissions inventory summary report: greenhouse gases, Tech. rep., Bay Area Air Quality Management District, San Francisco, CA, USA, 2015.

Dee, D. P., Uppala, S. M., Simmons, A. J., Berrisford, P., Poli, P., Kobayashi, S., Andrae, U., Balmaseda, M. A., Balsamo, G., Bauer, P., Bechtold, P., Beljaars, A. C. M., van de Berg, L., Bidlot, J., Bormann, N., Delsol, C., Dragani, R., Fuentes, M., Geer, A. J., Haimberger, L., Healy, S. B., Hersbach, H., Hólm, E. V., Isaksen, L., Kållberg, P., Köhler, M., Matricardi, M., McNally, A. P., Monge-Sanz, B. M., Morcrette, J.-J., Park, B.-K., Peubey, C., de Rosnay, P., Tavolato, C., Thépaut, J.-N., and

Vitart, F.: The ERA-Interim reanalysis: configuration and performance of the data assimilation system, Q. J. Royal Meteorol. Soc., 137, 553–597, doi:10.1002/qj.828, 2011.

de Foy, B.: City-level variations in NO_x emissions derived from hourly monitoring data in Chicago, Atmos. Environ., 176, 128–139, doi:10.1016/j.atmosenv.2017.12.028, 2018.

Gurney, K. R., Razlivanov, I., Song, Y., Zhou, Y., Benes, B., and Abdul-Massih, M.: Quantification of fossil fuel CO_2 emissions on the building/street scale for a large U.S. city, Environ. Sci. Technol., 46, 12194–12202, doi:10.1021/es3011282, 2012.

Harley, R. A., Marr, L. C., Lehner, J. K., and Giddings, S., N.: Changes in motor vehicle emissions on diurnal to decadal time scales and effects on atmospheric composition, Environ. Sci. Technol., 39, 5356–5362, doi:10.1021/es048172+, 2005.

Jiménez, P. A., Dudhia, J., González-Rouco J. F., Montávez, J. P., García-Bustamante, E., Navarro, J., Vilà-Guerau de Arellano, J., and Muñoz-Roldán, A.: An evaluation of WRF's ability to reproduce the surface wind over complex terrain based on typical circulation patterns, J. Geophys. Res. Atmos., 118, 7651–7669, doi:10.1002/jgrd.50585, 2013.

Kim, J., Shusterman, A. A., Lieschke, K. J., Newman, C., and Cohen, R. C.: The BErkeley Atmospheric CO_2 Observation Network: field calibration and evaluation of low-cost air quality sensors, Atmos. Meas. Tech., 11, 1937–1946, doi:10.5194/amt-11-1937-2018, 2018.

Kort, E. A., Angevine, W. M., Duren, R., and Miller, C. E.: Surface observations for monitoring urban fossil fuel CO_2 emissions: minimum site location requirements for the Los Angeles Megacity, J. Geophys. Res. Atmos., 118, 1577–1584, doi:10.1002/jgrd.50135, 2013.

Lopez, M., Schmidt, M., Delmotte, M., Colomb, A., Gros, V., Janssen, C., Lehman, S. J., Mondelain, D., Perrussel, O., Ramonet, M., Xueref-Remy, I., and Bousquet, P.: CO, NO_x, and $^{13}CO_2$ as tracers for fossil fuel CO_2: results from a pilot study in Paris during winter 2010, Atmos. Chem. Phys., 13, 7343–7358, doi:10.5194/acp-13-7343-2013, 2013.

Maness, H. L., Thurlow, M. E., McDonald, B. C., and Harley, R. A.: Estimates of CO_2 traffic emissions from mobile concentration estimates, J. Geophys. Res. Atmos., 120, 2087–2102, doi:10.1002/2014jd022876, 2015.

McDonald, B. C., McBride, Z. C., Martin, E. W., and Harley, R. A.: High-resolution mapping of motor vehicle carbon dioxide emissions, J. Geophys. Res. Atmos., 119, 5283–5298, doi:10.1002/2013jd021219, 2014.

McKain, K., Wofsy, S. C., Nehrkorn, T., Eluszkiewicz, J., Ehleringer, J. R., and Stephens, B. B.: Assessment of ground-based atmospheric observations for verification of greenhouse gas emissions from an urban region, P. Natl. Acad. Sci. USA, 109, 8423–8428, doi:10.1073/pnas.1116645109, 2012.

McKain, K., Down, A., Raciti, S. M., Budney, J., Hutrya, L. R., Floerchinger, C., Herndon, S. C., Nehrkorn, T., Zahniser, M. S., Jackson, R. B., Phillips, N., and Wofsy, S. C.: Methane emissions from natural gas infrastructure and use in the urban region of Boston, Massachusetts, P. Natl. Acad. Sci. USA, 112, 1941–1946, doi:10.1073/pnas.1416261112, 2015.

Nathan, B., Lauvaux, T., Turnbull, J., and Gurney, K.: Investigations into the use of multi-species measurements for source apportionment of the Indianapolis fossil fuel CO_2 signal, Elem. Sci. Anth., 6, 21, doi:10.1525/elementa.131, 2018.

Newman, S., Xu, X., Gurney, K. R., Hsu, Y. K., Li, K. F., Jiang, X., Keeling, R., Feng, S., O'Keeffe, D., Patarasuk, R., Wong, K. W., Rao, P., Fischer, M. L., and Yung, Y. L.: Toward consistency between trends in bottom-up CO_2 emissions and top-down atmospheric measurements in the Los Angeles megacity, Atmos. Chem. Phys., 16, 3843–3863, doi:10.5194/acp-16-3843-2016, 2016.

Pacala, S. W., Breidenich, C., Brewer, P. G., Fung, I., Gunson, M. R., Heddle, G., Law, B., Marland, G., Paustian, K., Prather, M., Randerson, J. T., Tans, P., and Wofsy, S. C.: Verifying Greenhouse Gas Emissions: Methods to Support International Climate Agreements, The National Academies Press, Washington, D. C., 2010.

Patarasuk, R., Gurney, K. R., O'Keeffe, D., Song, Y., Huang, J., Preeti, R., Buchert, M., Lin, J. C., Mendoza, D., and Ehleringer, J. R.: Urban high-resolution fossil fuel CO_2 emissions quantification and exploration of emission drivers for potential policy applications, Urban Ecosyst., 19, 1013–1039, doi:10.1007/s11252-016-0553-1, 2016.

Pugliese, S. C., Murphy, J. G., Vogel, F. R., Moran, M. D., Zhang, J., Zheng, Q., Stroud, C. A., Ren, S., Worthy, D., and Broquet, G.: High-resolution quantification of atmospheric CO_2 mixing ratios in the Greater Toronto Area, Canada, Atmos. Chem. Phys., 18, 3387–3401, doi:10.5194/acp-18-3387-2018, 2018.

Shusterman, A. A., Teige, V. E., Turner, A. J., Newman, C., Kim, J., and Cohen, R. C.: The BErkeley Atmospheric CO_2 Observation Network: initial evaluation, Atmos. Chem. Phys., 16, 13449–13463, doi:10.5194/acp-16-13449-2016, 2016.

Snyder, E. G., Watkins, T. H., Solomon, P. A., Thoma, E. D. Williams, R. W., Hagler, G. S. W., Shelow, D., Hindin, D. A., Kilaru, V. J., and Preuss, P. W.: The changing paradigm of air pollution monitoring, Environ. Sci. Technol., 47, 11369–11377, doi:10.1021/es4022602, 2013.

Turnbull, J. C., Sweeney, C., Karion, A., Newberger, T., Lehman, S. J., Tans, P. P., Davis, K. J., Lauvaux, T., Miles, N. L., Richardson, S. J., Cambaliza, M. O., Shepson, P. B., Gurney, K., Patarasuk, R., and Razlivanov, I.: Toward quantification and source sector identification of fossil fuel CO_2 emissions from an urban area: Results from the INFLUX experiment, J. Geophys. Res. Atmos., 120, 292–312, doi:10.1002/2014jd022555, 2015.

Turner, A. J., Shusterman, A. A., McDonald, B. C., Teige, V., Harley, R. A., and Cohen. R. C.: Network design for quantifying urban CO_2 emissions: assessing trade-offs between precision and network density, Atmos. Chem. Phys., 16, 13465–13475, doi:10.5194/acp-16-13465-2016, 2016.

United Nations, Human Settlement Programme: Hot Cities: Battle-Ground for Climate Change, 2011.

United Nations, Framework Convention on Climate Change: Adoption of the Paris Agreement, 21st Conference of the Parties, Paris, 2015.

United States Environmental Protection Agency, 2017 and Later Model Year Light-Duty Vehicle Greenhouse Gas Emissions and Corporate Average Fuel Economy Standards, Washington, D.C., 2012.

Verhulst, K. R., Karion, A., Kim, J., Salameh, P. K., Keeling, R. F., Newman, S., Miller, J., Sloop, C., Pongetti, T., Rao P., Wong, C., Hopkins, F. M., Yadav, V., Weiss, R. F., Duren, R. M., and Miller, C. E.: Carbon dioxide and methane measurements from the Los Angeles Megacity Carbon Project – Part 1: calibration, urban enhancements, and uncertainty estimates, Atmos. Chem. Phys., 17, 8313–8341, doi:10.5194/acp-17-8313-2017, 2017.

Wu, K., Lauvaux, T., Davis, K. J., Deng, A., Lopez Coto, I., Gurney, K. R., and Patarasuk, R.: Joint inverse estimation of fossil fuel and biogenic CO_2 fluxes in an urban environment: An observing system simulation experiment to assess the impact of multiple uncertainties, Elem. Sci. Anth., 6, doi:10.1525/elementa.138, 2018.

Zhu, Y., Kuhn, T., Mayo, P., and Hinds, W. C.: Comparison of daytime and nighttime concentration profiles and size distributions of ultrafine particles near a major highway, Environ. Sci. Technol., 40, 2531–2536, doi:10.1021/es0516514, 2006.

Figure 1. Map of BEACO$_2$N node locations (black dots). Nodes used in this study are labeled. Map data © 2017 Google

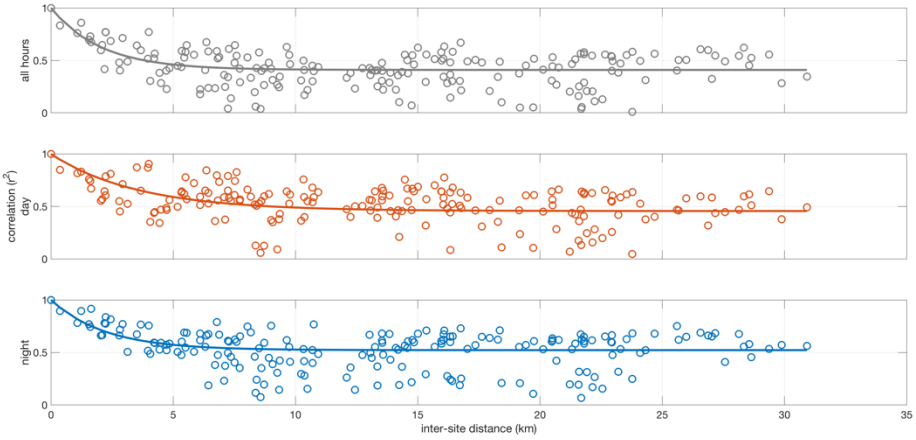

Figure 2. Optimal correlation coefficients for every possible pairing of summer 2017 sites as a function of their separation distance during all hours (top), daytime hours (1100–1800 LT, middle), and nighttime hours (2100–0400 LT, bottom). Solid lines show exponential decay of the correlation coefficients.

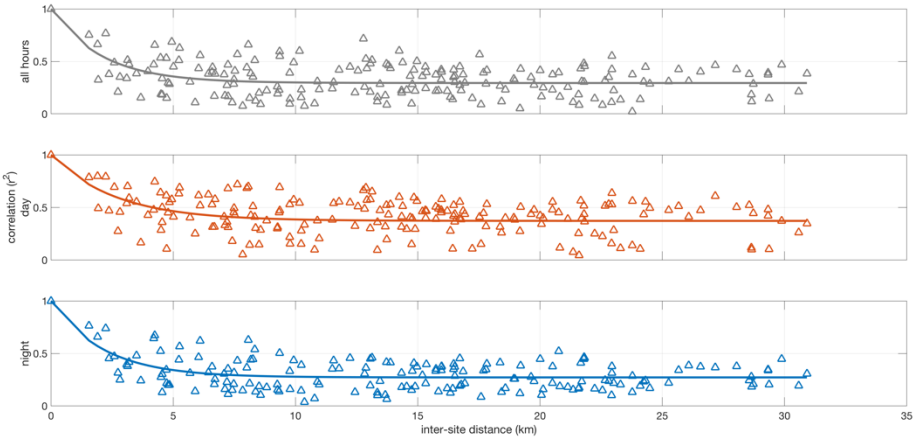

Figure 3. Optimal correlation coefficients for every possible pairing of winter 2017 sites as a function of their separation distance during all hours (top), daytime hours (1100–1800 LT, middle), and nighttime hours (2100–0400 LT, bottom). Solid lines show exponential decay of the correlation coefficients.

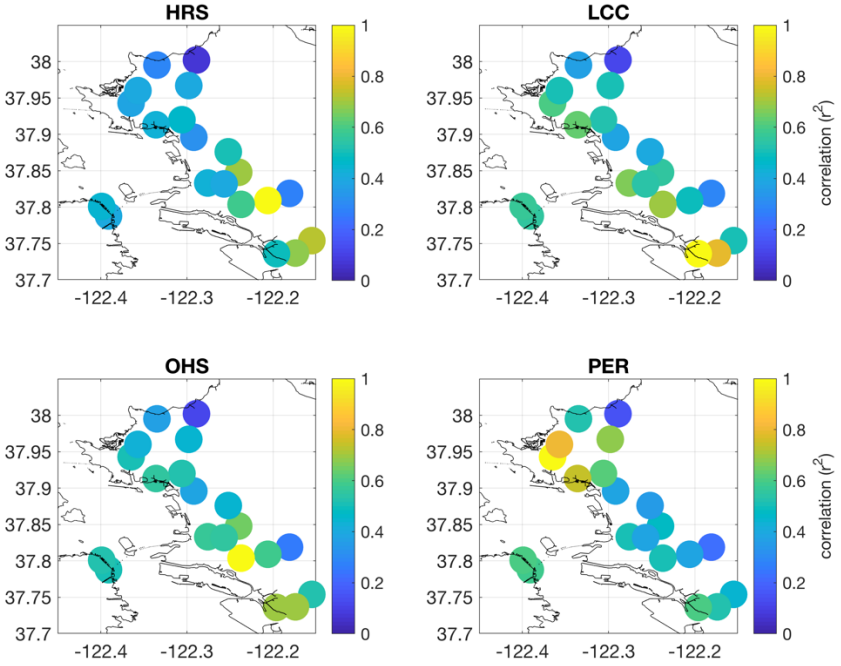

Figure 4. Optimal correlation coefficients representing network-wide correlation with 5-minute mean total CO_2 concentrations at four representative sites during daytime hours (1100–1800 LT) of winter 2017. Yellow spot ($r^2 = 1$) on each subplot shows the location of the site with which the correlation is examined.

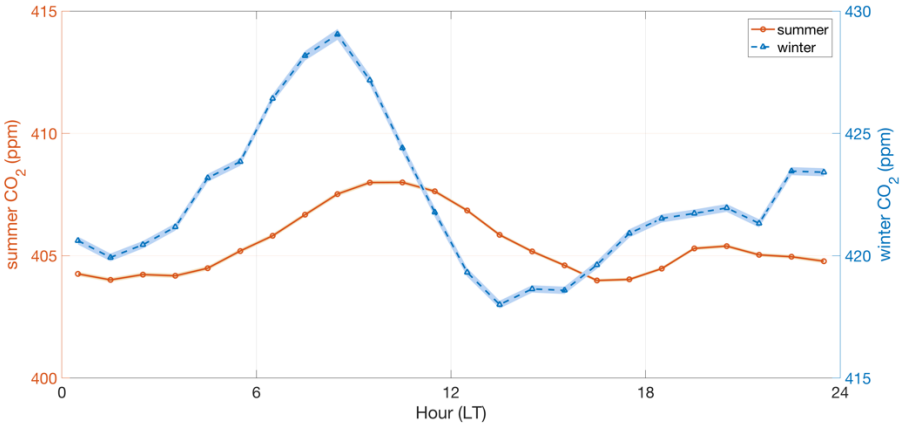

Figure 54. Hourly median values of the network-wide, regional CO_2 signals calculated for summer (orange) and winter (blue) periods in 2017. Lighter colored curves indicate the standard error; note the difference in y-scale.

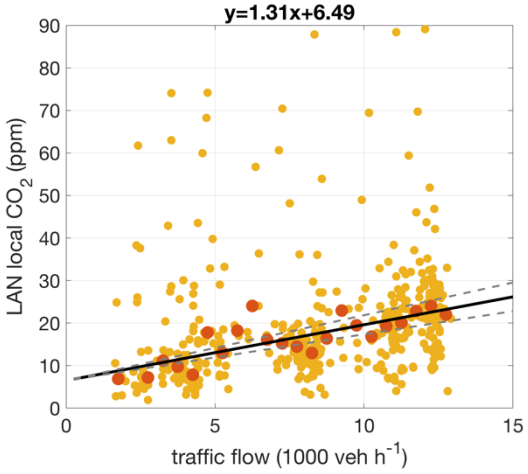

Figure 65. Morning (0400–0800 LT) local summertime CO_2 concentrations at LAN shown as a function of nearby highway traffic flow. Darker points indicate the median CO_2 concentration observed in each 500 veh h^{-1} traffic flow increment; black solid line indicates the linear regression through the binned medians (equation given above plot) and gray dashed lines show the uncertainty in the regression slope.

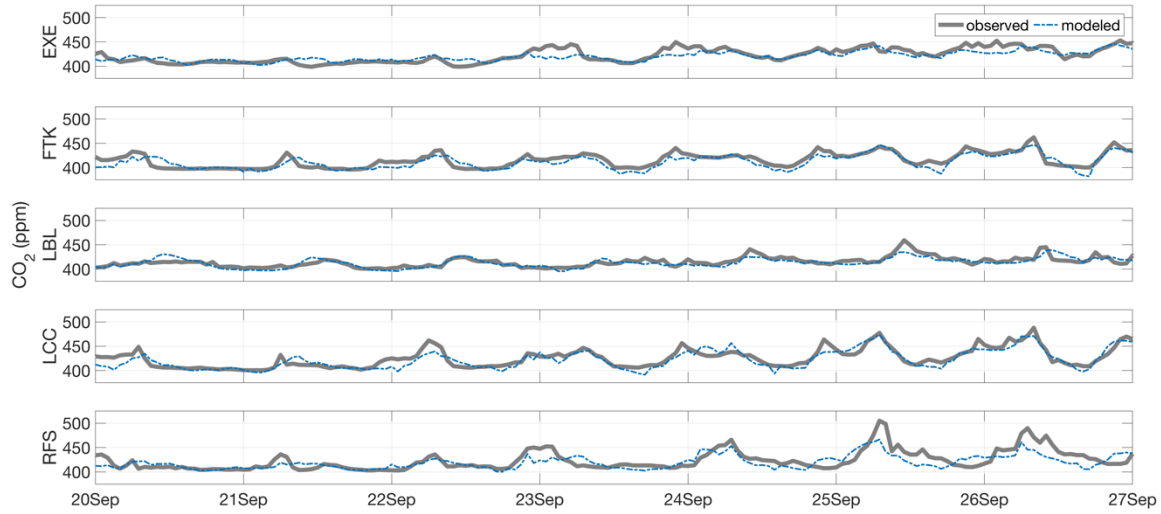

Figure 7. Representative week of total CO_2 concentrations observed (thick gray curve) and modeled (dashed blue curve) at five sites using a multiple linear regression approach based on de Foy (2018).

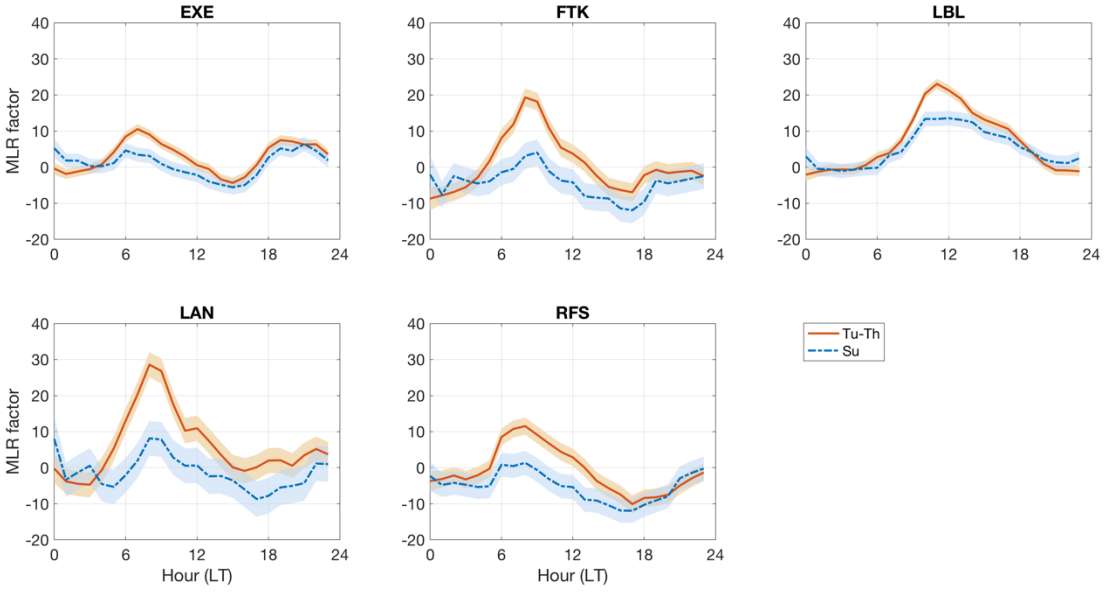

Figure ~~8~~6. Multiple linear regression coefficients for five sites derived for each hour of the day on Tuesdays through Thursdays (orange solid line) and Sundays (blue dashed line) between 15 February 2017 and 15 February 2018.

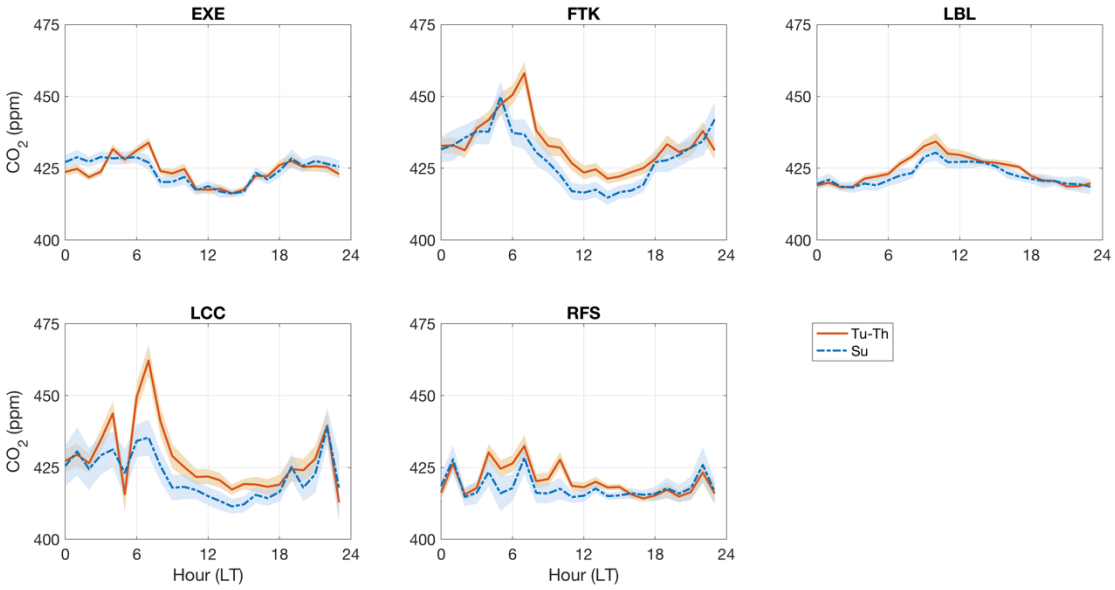

Figure 9. Hourly median CO_2 concentrations observed at five sites on Tuesdays through Thursdays (orange solid line) and Sundays (blue dashed line) between 15 February 2017 and 15 February 2018; lighter curves indicate the standard error in the medians.

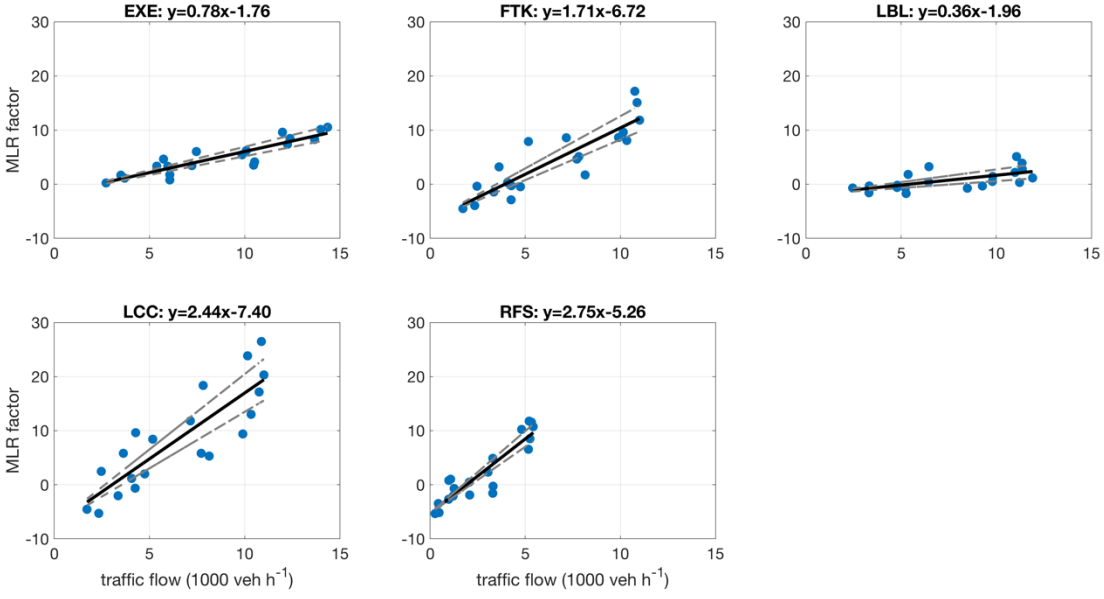

Figure 10. Morning (0400–0800 LT) multiple linear regression coefficients shown as a function of summertime traffic flow; black solid lines indicate the linear regression through the ~~binned medians~~MLR factors (equations given above each subplot) and gray dashed lines show the uncertainty in the regression slope.

SITE CODE	LAT (º N)	LON (º E)	TRAFFIC MONITOR IDs	DISTANCE FROM HIGHWAY (m)
ALB*	37.896	-122.292	401052, 402062	1390
BAM	37.788	-122.391	402815, 404920	170
BOD*	37.754	-122.156	401857, 401858	300
CHA	37.819	-122.181	400302, 400308	1720
COL	38.002	-122.289	401230, 401269	510
CPS*	37.848	-122.240	402201, 402202	220
DEJ†	37.933	-122.338	400361, 400445	950
EXB†	37.802	-122.397	402815, 404920	1570
EXE	37.801	-122.399	402815, 404920	1580
FTK	37.737	-122.173	JJAS: 400442, 400955 NDJ: 400608, 400793	1350
HRS*	37.809	-122.205	400302, 400308	700
LAN†	37.794	-122.263	400835, 408138	40
LBL	37.876	-122.252	400176, 400728	3090
LCC	37.736	-122.196	JJAS: 400442, 400955 NDJ: 400608, 400793	220
MAD†	37.928	-122.299	400819, 401558	1850
MAR†	37.863	-122.314	400176, 400728	950
MTA	37.995	-122.335	400538, 400976	2040
NOC*	37.833	-122.276	401211, 401513	750
NYS†	37.928	-122.359	400359, 400734	380
OHS*	37.804	-122.236	400261, 401017	160
PDS*	37.831	-122.257	400224, 401381	800
PER	37.943	-122.365	400639, 400738	1790
PTL	37.920	-122.306	400819, 401588	970
RFS	37.913	-122.336	400202, 400675	760
RHS†	37.953	-122.347	401228, 406660	1530
SHL	37.967	-122.298	416774, 416790	2030
SPB*	37.960	-122.357	401894, 401895	2280
STW†	37.990	-122.291	400313, 400902	500

Table 1.~~:~~ List of site geo-coordinates, relevant traffic monitor IDs, and approximate distances from a highway. Asterisks indicate sites with data available in winter 2017 only; daggers indicate sites with data available in summer 2017 only.

SITE CODE	MLR VARIABLE					
	TIME OF YEAR	DAY OF WEEK	BLH	WIND	T	HUMIDITY
EXE	0.271	0.031	0.130	0.028	0.031	--
FTK	0.413	0.050	0.088	0.024	--	0.010
LBL	0.230	0.156	0.052	0.028	0.008	0.024
LCC	0.353	0.062	0.177	0.021	--	--
RFS	0.316	0.052	0.082	0.029	0.006	--

Table 2. Explanatory variables included in the multiple linear regression analysis of each site; values indicate the correlation coefficient increase achieved by subsequent inclusion of each variable.

Supplement of

Observing local CO_2 sources using low-cost, near-surface urban monitors

Alexis A. Shusterman et al.

Correspondence to: Ronald C. Cohen (rccohen@berkeley.edu)

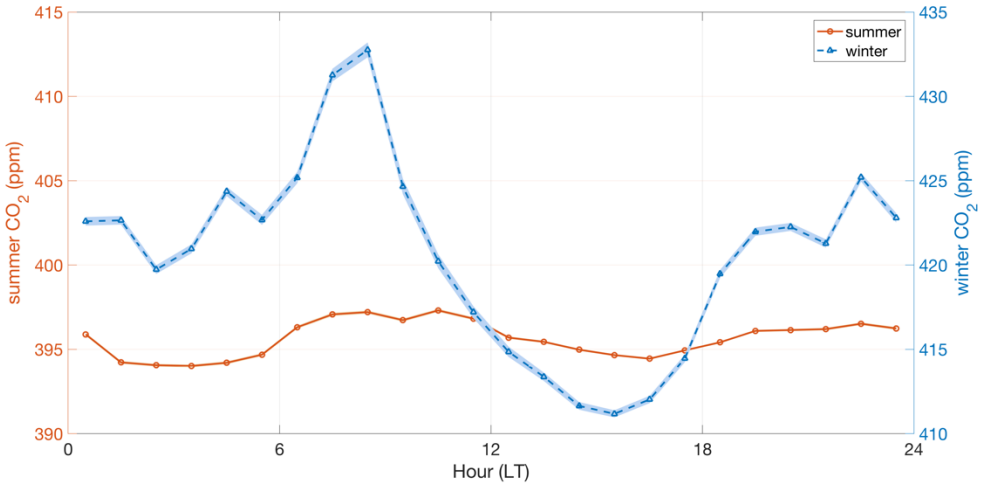

Figure S1: Hourly median values of the network-wide, regional CO_2 signals calculated for summer (orange) and winter (blue) periods in 2013. Lighter colored curves indicate the standard error; note the difference in y-scale.

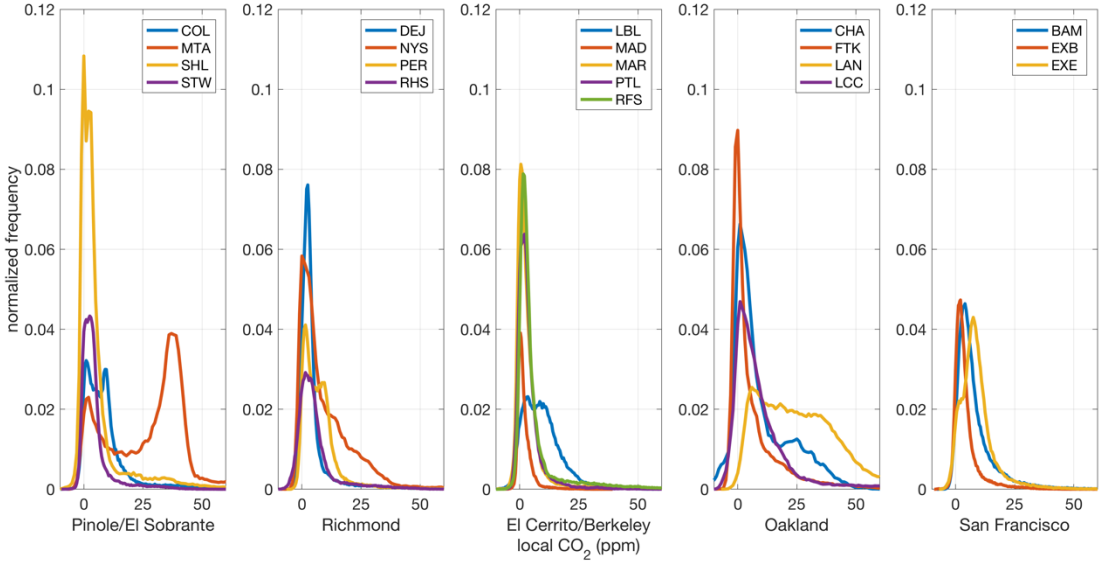

5

Figure S2: Normalized distributions of local CO_2 concentrations observed during summer 2017.

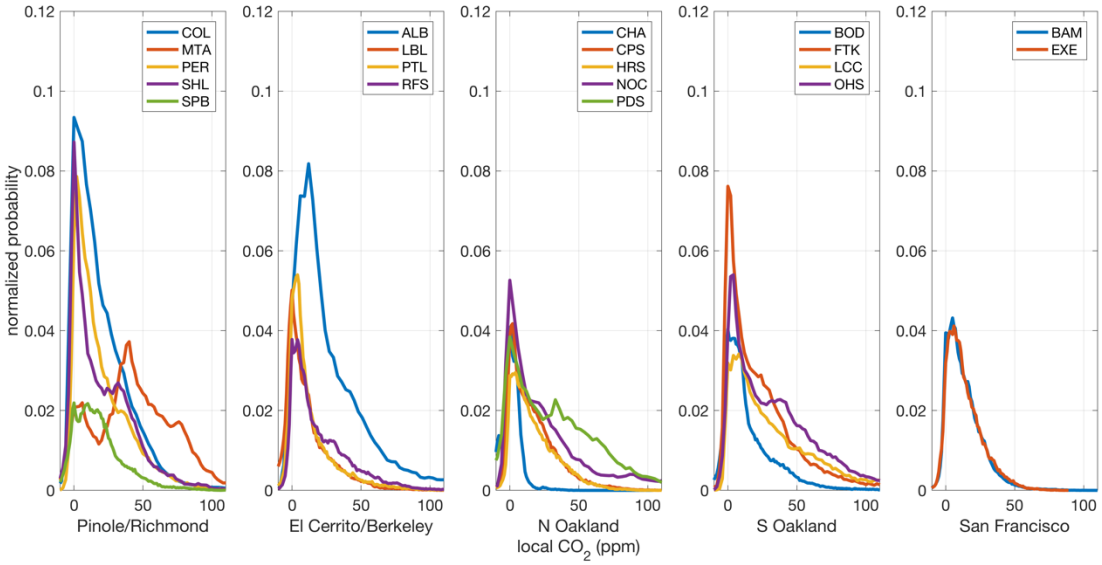

Figure S3: Normalized distributions of local CO_2 concentrations observed during winter 2017.

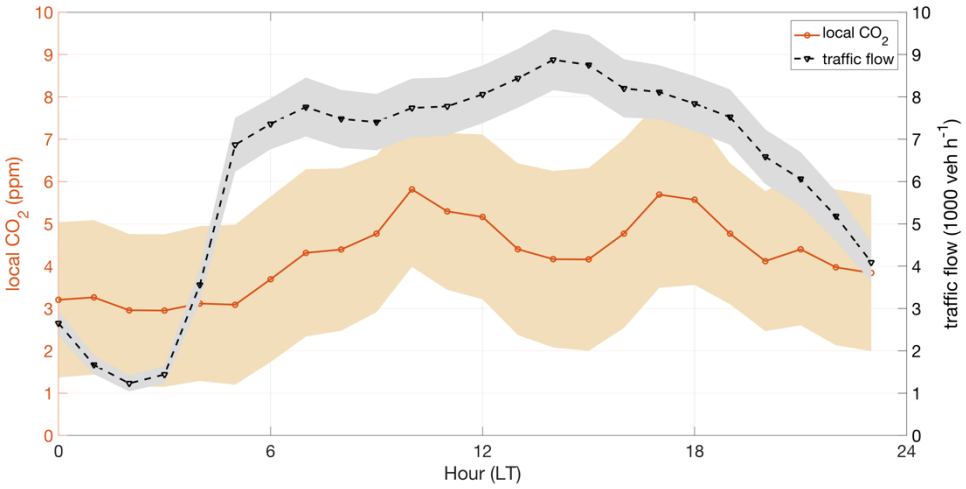

Figure S4: Hourly network-wide median local CO_2 and traffic flows observed during summer 2017. Lighter colored curves indicate standard error.

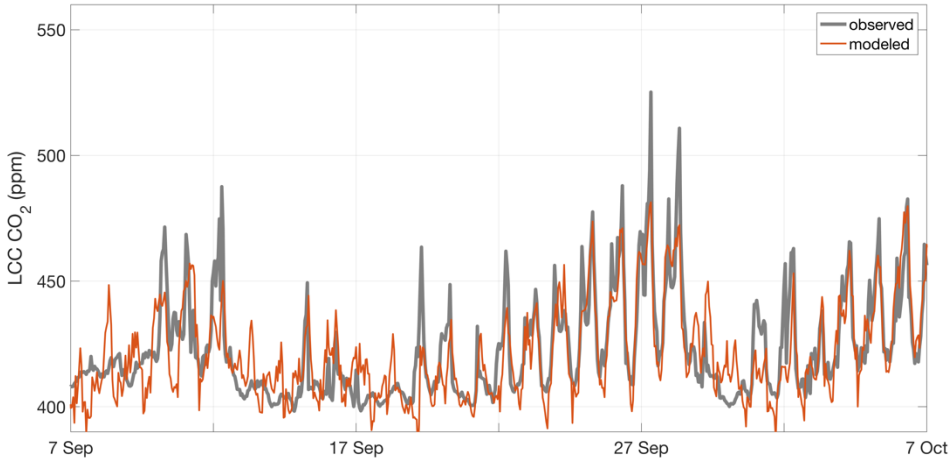

~~**Figure S5: Representative month of total CO_2 concentrations observed (thick gray curve) and modeled (thin orange curve) at LCC site using a multiple linear regression approach based on de Foy (2018).**~~

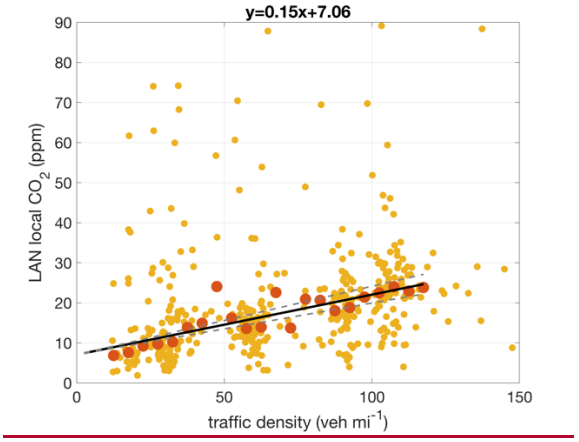

Figure S5. Morning (0400–0800 LT) local summertime CO_2 concentrations at LAN shown as a function of nearby highway traffic density. Darker points indicate the median CO_2 concentration observed in each 5 veh mi^{-1} traffic density increment; black solid line indicates the linear regression through the binned medians (equation given above plot) and gray dashed lines show the uncertainty in the regression slope.

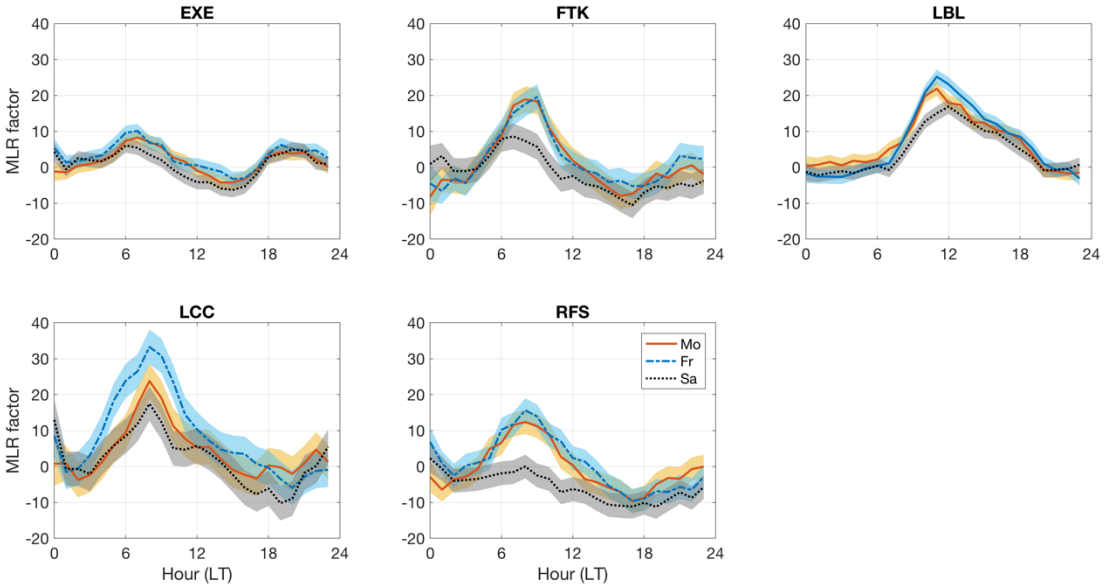

Figure S6. Multiple linear regression coefficients for five sites derived for each hour of the day on Mondays (orange solid line), Fridays (blue dashed line), and Saturdays (black dotted line) between 15 February 2017 and 15 February 2018.